THE JOURNAL
OF
CHEMICAL PHYSICS

VOLUME 12, NUMBER 3 MARCH, 1944

Infra-Red Absorption of Solid Ammonium Chloride and Ammonium Bromide*

CLIFFORD BECK**
University of North Carolina, Chapel Hill, North Carolina
(Received January 7, 1944)

According to theoretical considerations based on specific heat, dielectric constant, coefficient of expansion, and other properties, the molecules of the solid ammonium halides, at room temperature, are thought to possess rotatory motion. This rotation is expected not to exist at temperatures below the transition temperature; namely, −30.4°C for the chloride and −37.9°C for the bromide. Molecular rotation, if present, should give rise to rotational fine structure superposed on the infra-red vibrational bands of the salts. Previous workers found evidence of this, but have not resolved the fine structure. The present investigation was undertaken in the hope of resolving this fine structure, if any, and studying the changes in it resulting from lowering the temperature below the transition point. Fine structure in the 5.6-μ vibrational band of ammonium chloride and ammonium bromide was resolved. This structure was of the order of magnitude expected if the NH_4 group rotating in the molecule were responsible for the fine structure. The fine structure existed practically unaltered to temperatures down to −20°C. There was considerable change between −20°C and −45°C, but then the altered fine structure persisted down to at least −60°C with little additional change.

INTRODUCTION

THE study of the infra-red absorption spectra of many gases under high dispersion has yielded much valuable information about the structure and behavior of their molecules. The infra-red absorption bands of solids have not been studied as extensively with instruments of high resolving power, though such investigations should also yield valuable information.

Of particular interest are those crystals in which the molecules are believed to undergo some form of rotation. Typical of these are the ammonium halides, for which theory[1] predicts the existence of rotational motion of the NH_4 group at room temperature. A review of the literature† reveals that experiments on specific heats, dielectric constants, coefficients of expansion, crystal structure, and Raman spectra do not contradict the predicted molecular rotation, but neither do they furnish proof of its existence. However, the most recent report[2] of the numerous investigations of the infra-red spectra of the ammonium halides furnishes some evidence of the presence of rotational fine structure in the 5.6-μ vibrational band of the ammonium salts. Pohlman, with a prism spectrometer, studied the infra-red bands at temperatures both above and below the lower transition points (at, or near, which rotation is expected to cease—with decreasing temperature). He obtained differences in the bands at the two temperatures, but the resolving power of his instruments was not sufficiently great to allow conclusions regarding the rotatory state of the molecules to be drawn.

The present investigation, employing a grating spectrometer of higher resolving power than

* Experiments performed in 1942.
** Now a member of the scientific staff of Columbia University.
[1] L. Pauling, Phys. Rev. **36**, 430 (1930).
† A short bibliography of pertinent papers is attached to the end of this report.
[2] R. Pohlman, Zeits. f. Physik **79**, 394 (1932).

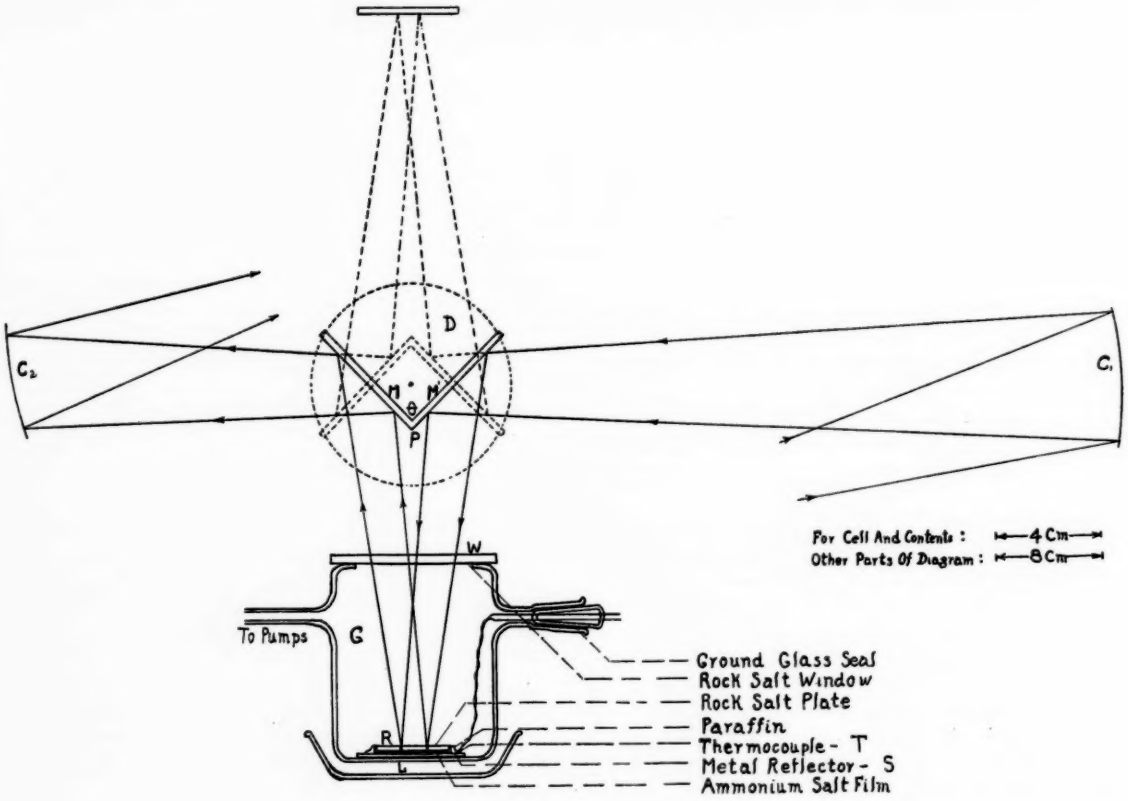

FIG. 1.

those used in the previous studies, was undertaken in the hope of resolving any rotational fine structure present in the vibrational bands of ammonium chloride and ammonium bromide at room temperature, and determining what changes occurred in this fine structure at temperatures below the transition point (−30.4°C for the chloride and −37.9°C for the bromide). There is a report in the literature of a successful experiment similar to the proposed one. Shearin,[3] using a grating spectrometer, was able to resolve clearly the fine structure in the near infra-red vibrational band of HCL after Hettner,[4] in a previous experiment with a prism instrument of lower resolving power, had found evidence of the existence of the rotational fine structure.

At room temperature in this investigation, attention was directed to the 5.6-μ and 7-μ bands of the two salts. The 3.2-μ bands were inaccessible with the apparatus used here, because of high CO_2 and water vapor absorption of the atmosphere at that wave-length. At low temperatures, attention was focused on the 5.6-μ band of ammonium bromide only. The latter procedure was adopted because Pohlman's investigation, and exploratory experiments in the present investigation, indicated (1) that little change occurred in the 7-μ bands in going to low temperature, and (2) that similar changes in the 5.6-μ bands of both ammonium chloride and ammonium bromide were to be expected in going to temperatures below the transition temperature. The ammonium bromide was chosen for this work.

This investigation, therefore, was divided into two parts. The first dealt with experiments at room temperature, which included studies of the 5.6-μ and 7-μ bands of ammonium chloride and ammonium bromide. The second part consisted of a study of the 5.6-μ band of ammonium bromide at four different temperatures ranging from 27°C to −60°C.

[3] P. E. Shearin, Phys. Rev. **48**, 299 (1935).
[4] G. Hettner, Zeits. f. Physik **78**, 141 (1932).

I. APPARATUS AND PROCEDURE

A. Spectrometer and Optical Path at Room Temperature

The conventional type of infra-red grating spectrometer used in these experiments was calibrated by Shearin and Plyler[5] in 1938, and was rechecked during the present experiments by use of well-known CO_2 and water vapor bands. The infra-red source was a Nernst glower, operating on 110 volts a.c. in series with a variable resistor by means of which the current was adjusted to 0.3 ampere.

For room temperature experiments, the radiation, after passing through a 30° rocksalt foreprism, was focused on, and passed through, a thin film of the solid ammonium salt under investigation. The latter was deposited on a plate of rocksalt which could be moved vertically out of the beam to allow for zero readings. After traversing the film and plate, the beam passed through a shutter into an insulated housing enclosing the grating (2060 lines per inch) and the vacuum-thermopile detector. The current from the detector, after amplification by a Moll thermorelay, went to a galvanometer from whose mirror a spot of light was reflected some four meters to a translucent scale on which readings were made. The slits in the optical path were 0.5 mm in width for all data, giving an equivalent slit-width of 0.012μ.

For each setting of the grating angle, the radiation first passed through the rocksalt plate and film of ammonium salt. This plate was then moved out of the beam and automatically replaced by a similar rocksalt plate having no deposited film. The ratio of the galvanometer deflection with the film in the beam to the deflection with the film out of the beam gave the percentage transmission of the ammonium salt for that wave-length. Prior to depositing the film on the plate, adjustments were made so that the beam in alternately traversing the two plates produced the same galvanometer deflection.

B. Low Temperature Apparatus

For the low temperature experiments the optical path was altered to the form shown in Fig. 1. The support for the rocksalt plates used in the room temperature experiments was replaced by two front-surfaced, plane mirrors M and M' (Fig. 1) mounted on a vertical disk D which could be rotated about its horizontal axis, the axis being perpendicular to the beam. The mirrors were mounted with their planes perpendicular to the face of the disk, with one pair of their ends P in contact, and with a dihedral angle of 95° between them. Directly below the mirrors was placed an evacuated cell G containing the rocksalt plate R which had the film under investigation deposited on its bottom face. The rocksalt plate R rested, with the film of ammonium halide downward, on a metal reflector S of polished stainless steel, to which it was firmly held by paraffin around the edges. The top of the cell was closed by a rocksalt window W.

The concave mirror C_1 was adjusted so that, when the plane mirrors were turned with P pointing downwards, the light beam followed the arrows from C_1 to M' to a focus on the reflector S; thence to M, C_2, and the detector. In the cell it passed twice through the rocksalt plate and the film of ammonium salt. When the disk was rotated through 180° so that P pointed upwards, the beam traversed a similar path from C_1 to C_2, but one not containing the ammonium salt and the two rocksalt plates R and W. The ratio of the deflections of the galvanometer as the beam alternately travelled the two paths gave the percentage absorption of the film for that wave-length. Prior to depositing the film the apparatus was adjusted so that (with R and W in place) the beam, in alternately traversing the two paths, produced equal galvanometer deflections.

Close beside the plate of rocksalt R a copper constantan thermocouple T was securely fixed to the steel reflector. It is estimated that temperatures of the film, indicated by the nearby thermocouple, are not in error by more than ± 3°C. Beneath the steel reflector in the cell a thin layer of solder furnished thermal contact with the glass bottom of the cell. Underneath the cell was placed a small, shallow dish containing the cooling agents used to control the temperature of the film.

[5] E. K. Plyler and P. E. Shearin, J. Opt. Soc. Am. **28**, 61 (1938).

C. Preparation of Films

The method of preparing films found most satisfactory consisted in suspending the rocksalt plate horizontally, face-downwards, inside a large-mouth flask, evacuated to about 10^{-3} cm of mercury. A small flame underneath the flask caused part of the ammonium salt crystals, thinly scattered on the bottom of the flask, to vaporize. Some of the vapor condensed on the rocksalt

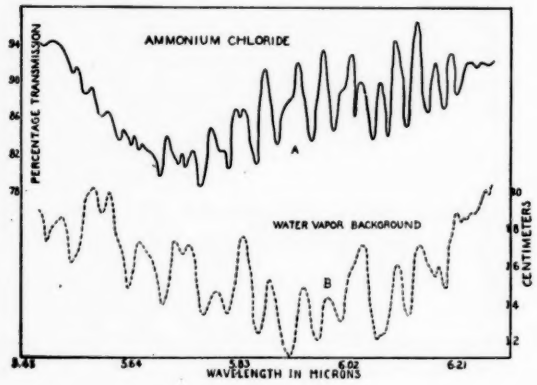

FIG. 2.

plate. Heating continued until enough vapor condensed on the plate to give a film of the desired opacity. Only films having a percentage transmission of 80 percent$\pm$2 percent at the center of the 5.6-μ band of that salt were used in these experiments. Microscopic examination revealed that the crystals in the films obtained by this "vacuum" method were so closely packed that it was impossible to determine where one crystal stopped and the next began. Thus, a practically continuous layer of salt was presented to the incident light, rather than many individual scattering particles.

II. RESULTS

A. Room Temperature

On three ammonium chloride films, deposited by the vacuum method described above, five complete runs through the 5.6-μ band and three through the 7-μ band were made. In each run, readings were taken at intervals of one minute of arc on the grating circle, corresponding to 0.007μ.

The percentage of incident radiation transmitted by the halide film as a function of wavelength is shown in Fig. 2*A* for the 5.6-μ band. The fine structure lines shown in Fig. 2 were reproducible in successive experiments, with only small differences in depth of the absorption lines and irregularities on the higher percentage transmission "peaks" (see Section III B). The wavelengths and wave numbers of the prominent fine structure lines appearing in the 5.6-μ band of ammonium chloride are listed in columns 1 and 2, respectively, of Table I. Column 3, $\Delta\nu$, is the difference, in wave numbers, between the successive prominent fine structure lines.

The intensity of the 7-μ band of ammonium chloride (Fig. 3*A*) is so great that at the band center almost no radiation penetrates a film which allows 96 percent transmission on the sides of the band. No fine structure is present, but a few minor irregularities appear on the sides of the band.

In Fig. 4 the 5.6-μ band of ammonium bromide is shown. It is noticed that the intense, fairly regularly spaced fine structure lines throughout the band are more prominent than in the corresponding chloride band. The average spacing of these lines is about the same as in the chloride band. (See Tables I and II.) Between the intense lines, on the peaks of the curve, there are irregularities which indicate a much narrower, unresolved, fine structure similar to, though more pronounced than, that found in the corresponding chloride band. It was not possible to determine this smaller fine structure accurately with the instrument used here. Table II gives the information for the ammonium bromide corresponding to that listed in Table I for the chloride.

TABLE I. Fine structure lines of the 5.6-μ band of NH_4Cl.

Wave-length microns	Wave numbers cm^{-1}	$\Delta\nu$ cm^{-1}	
5.69	1760		
5.76	1740	20	
5.81	1723	17	
5.86	1708	15	
5.90	1696	12	Average
5.96	1680	16	$\Delta\nu=15.2$ cm^{-1}
6.00	1667	13	
6.06	1650	17	
6.12	1636	14	
6.16	1624	12	
6.19	1608	16	

The 7-μ band of ammonium bromide (Fig. 5) was found to be similar in width and intensity to the corresponding chloride band. However, there was some difference in that the bromide band showed some very narrow fine structure of low intensity and a shape on the long wave-length side somewhat different from that shown in the corresponding band of the chloride.

B. Ammonium Bromide at Various Temperatures

Only one film of ammonium bromide was used in these experiments, and all data were taken on the same day. On this film, two sets of data were taken through the 5.6-μ band at each of four temperatures, in the order named: 27°C, −20°C, −45°C, −60°C. At the end of the last run the temperature was allowed to return to 27°C and another set of data was taken (which duplicated almost exactly the previous data at 27°C). All readings were taken at 2-minute intervals 0.014μ on the grating circle.

The two curves in Fig. 6 show the results obtained. The dotted curve represents the absorption at 27°C and −20°C: The fine structure at these two temperatures was practically identical. This dotted curve appears slightly different from the curve in Fig. 4, which was also obtained at 27°C. The difference is due to the procedure of taking readings at 2-minute intervals (or 0.0014μ) for the curve in Fig. 6, which fails to reveal some of the less prominent lines shown in the curve of Fig. 4 (for which readings were taken at 1-minute intervals). The solid curve (Fig. 6) shows the absorption at −45°C and −60°C, for it was found that at both of these temperatures the band possessed the same fine structure. The alteration in fine structure occurred between −20° and −45°C.

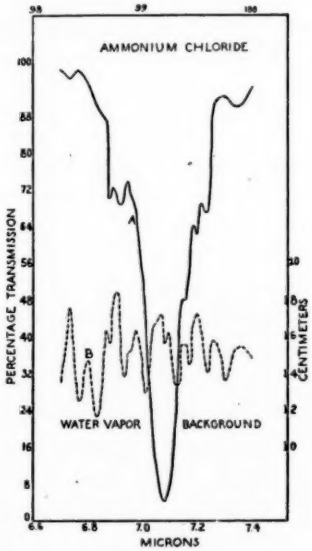

FIG. 3.

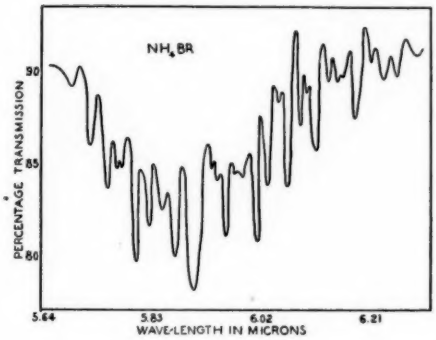

FIG. 4.

Three points are to be noticed. First, the fine structure is much decreased in intensity at the lower temperature, but is still present, at the same wave-lengths. Second, the over-all shape of the band at the lower temperature is sharper and the charge is such that instruments of low resolving power would indicate a slight apparent shift of the band to shorter wave-lengths. Third, as mentioned above, the alteration takes place between −20°C and −45°C, a temperature range which includes the transition temperature of this salt (−37.9°C).

III. DISCUSSION OF RESULTS

A. Water Vapor in Atmosphere

The study of the infra-red spectra of the ammonium salts was complicated by the presence of numerous fine structure lines of the broad water vapor band having a center at 6.26μ.[6] The radiation from the Nernst glower has practically uniform intensity throughout this region. But the water vapor caused the galvanometer deflections through the air to vary from 4 to 30 centimeters, depending on the humidity and on the proximity of the grating setting to a

[6] E. K. Plyler and W. W. Sleator, Phys. Rev. **37**, 1493 (1931).

water vapor line. This explains the necessity of making two galvanometer readings for each wave-length in order to obtain the percentage transmission: one, that resulting when the radiation traversed the air path alone; the other,

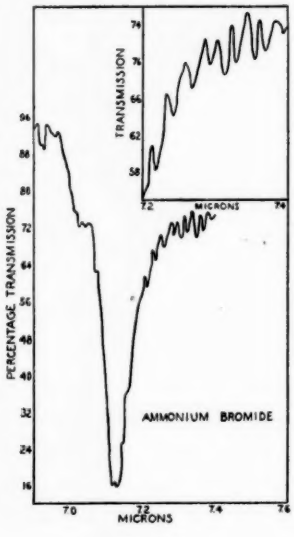

FIG. 5.

when both the air path and halide film were traversed. By simply plotting the air deflections of the galvanometer from any set of data as a function of wave-length the water vapor absorption spectrum could be shown (curve *B*, Fig. 2 and curve *B*, Fig. 3).

The wave-length spacing of the water fine structure is of the same order of magnitude as that of the ammonium chloride shown in curve *A* (Fig. 2). At first glance one might suspect that the apparent fine structure in the chloride band could be a result of the water vapor structure. But a careful scrutiny shows that there is no consistent correlation between peaks or dips on the two curves, as would be the case if the apparent fine structure on the halide curve were a result of the water vapor structure. Also the decidedly different structure of the NH_4Cl band on the low wave-length side, where the water structure is about the same, indicates that the water vapor is not responsible for the structure appearing on the NH_4Cl band. A similar bit of evidence comes from Fig. 3, which shows the band of NH_4Cl at 7μ, where the water structure (curve *B*) is more pronounced than at 5.6μ. But there is no fine structure on the chloride band. Finally, it was found that similar fine structure of the ammonium salts was obtained on days of quite different absolute humidity. Thus it appears that the water vapor, though troublesome, did not affect the absorption spectra obtained for the ammonium salts.

B. Errors and Accuracy

For any setting of the grating angle, consecutive measurements of percentage transmission of the ammonium salt agreed within ± 0.5 percent. The chief discrepancy in the data from film to film, or between different experiments on the same film, resulted from the inability to reproduce grating-angle settings exactly. With the aid of a low power microscope, it was possible to reproduce grating angle settings to within an estimated maximum error of 6 seconds of arc, which corresponds to a possible variation of 0.0015μ in wave-length. This is about 7 percent of the equivalent slit-width. If intense, closely spaced, fine structure lines were present, then an error of this magnitude in wave-length setting could cause an appreciable difference in the percentage transmission. This is apparently the case in the $5.6\text{-}\mu$ bands, for, though successive measurements of transmission were constant for a given grating setting, the measurements frequently were not exactly the same when the grating angle was reset after having been moved. Thus, there was some uncertainty as to the absolute depth of a given line and the finer details on the "peaks" of the curves.

However, the prominent fine structure lines

TABLE II. Fine structure lines of the $5.6\text{-}\mu$ band of NH_4Br.

Wave-length microns	Wave numbers cm^{-1}	$\Delta\nu$ cm^{-1}	
5.71	1750		
5.75	1740	10	
5.80	1725	15	
5.87	1705	20	
5.91	1692	13	Average
5.96	1679	13	$\Delta\nu = 14.8\ cm^{-1}$
6.02	1660	19	
6.07	1648	12	
6.11	1636	12	
6.18	1618	18	
6.24	1602	16	

shown in the bands at room temperature were reproducible from film to film. And in the low temperature experiments, the difference in fine structure between $-20°C$ and $-45°C$ (Fig. 6) was of such magnitude that the small variations were negligible in comparison. The wave-lengths of the absorption lines are accurate to within about 0.006μ; approximately half the equivalent slit-width.

C. Room Temperature

The results of this investigation of the $7\text{-}\mu$ bands of ammonium chloride and ammonium bromide are in agreement with results of earlier investigations, and show little in addition. The irregularity on the long wave-length side of the $7\text{-}\mu$ band of the bromide is more clearly shown n this investigation, but the explanation of ts presence in the bromide band and its absence in the chloride band, or of the difference between the shapes of these corresponding bands of the two salts is not known.

The prominent fine structure in the $5.6\text{-}\mu$ band of the ammonium bromide (Fig. 4) appears to be of the same nature as the structure in the corresponding band of ammonium chloride (Fig. 2), because the lines are similar in spacing and arrangement. However, there are two distinct differences. First, the shorter wave-length side of the band in the chloride has more irregularity, and was less resolvable, while in the bromide the fine structure lines were present on both sides of the band. Second, on the peaks of the curves, between the narrow fine structure absorption lines, the curve for the bromide shows more irregularity than is found on the corresponding curve for the chloride. The crystal structures of the two salts at room temperature, as pointed out earlier, are believed to be identical, and the tetrahedral arrangement of the NH_4 radical in the crystals of both salts is assumed similar. The differences, therefore, in the fine structure of the corresponding band of the two salts are perhaps due to unequal influence of the different halogen atoms on the NH_4 radical in the respective crystals.

D. Low Temperature

It was hoped that examination of the fine structure of the $5.6\text{-}\mu$ bromide band both above and below the transition temperature would indicate whether or not rotation of the molecules was present at room temperature, and if so, whether this rotation ceased below the transition temperature. From the results obtained, if the resolved fine structure at the higher temperature is due to rotation, then the molecules continue to rotate below the transition temperature.

On the basis of a calculation of the kind outlined by Pohlman[2] for the fine structure obtained

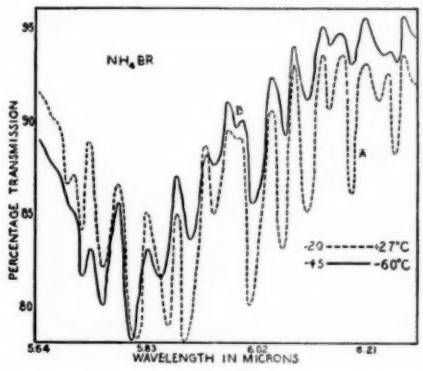

FIG. 6.

in NH_4NO_3, it is indicated that the fine structure obtained in the present investigation is due to rotation. We take

$$\Delta\nu = 15 \text{ cm}^{-1}$$

as the average spacing of the fine structure lines for the two salts, and assume an average wave-length

$$\lambda = 5.6\mu = 5.6\times10^{-4} \text{ cm}.$$

If one assumes that the rotation of the tetrahedral NH_4 radical is responsible for these lines, it follows that the moment of inertia is independent of the direction of the axis of rotation. From this, one obtains for the moment of inertia

$$I = \frac{h}{4\pi^2\Delta\nu} = 3.69\times10^{-40} \text{ g cm}^2.$$

Then, from the geometry of the tetrahedron, it follows that the $N-H$ distance indicated by these experiments is 0.913×10^{-8} centimeter. However, in this calculation, no consideration has been made of the possible influences of the neighboring atoms on the rotation groups. Therefore, the value stated above is to be taken as the

order of magnitude, and not as an absolute measure of the N−H distance in NH_4.

It is known from other studies of the structure of molecules that the value obtained here (0.913×10^{-8} cm) for the intermolecular distance is approximately correct. Therefore, the calculation above indicates that the infra-red fine structure of these two ammonium salts is due to rotation of the NH_4 group in the crystal. And the low temperature data indicate that this rotation continues, though quite altered, at temperatures below the transition temperature.

The author expresses his sincere thanks to Dr. Paul E. Shearin who suggested this investigation and gave unfailing interest and practical aid in the experiments, and to Dr. Nathan Rosen for his interest and helpful discussions.

BIBLIOGRAPHY

(1) T. E. Stern, "The symmetric spherical oscillator, and the rotational motion of homopolar molecules in crystals," Proc. Roy. Soc. London **130**, 551 (1930–31).

(2) J. Errera and H. Sack, "Dielectric constant of magnesium and yttrium platinocyanide crystals and the possibility of molecular rotation in solids," Trans. Faraday Soc. **30**, 687 (1934).

(3) J. Frenkel, "Rotation of dipole molecules in solid bodies," Acta Phys. Chem. U.S.S.R. **1**, 23 (1935).

(4) R. H. Fowler, "Rotations of molecules in solids," Proc. Roy. Soc. London **149**, 1 (1935).

(5) F. Simon, "Untersuchungen über die spezifische Wärme bei tiefen Temperaturen," Ann. d. Physik **68**, 241 (1922).

(6) F. Simon and R. Bergmann, "Messung der thermischen Ausdehnung in Gebiet der Anomalie," Zeits. f. physik. Chemie **B8**, 255 (1930).

(7) F. Simon, C. Simpson, and M. Ruhemann, "Untersuchungen über die spezifischen Wärmen bei tiefen Temperaturen," Zeits. f. physik. Chemie **129**, 339 (1927).

(8) G. Bartlett and I. Langmuir, "The crystal structures of the ammonium halides above and below the transition temperatures," J. Am. Chem. Soc. **43**, 84 (1921).

(9) A. Hettich, "Über den Tieftemperaturzustand der Ammoniumsalze," Zeits. f. physik. Chemie **A168**, 353 (1934).

(10) J. A. A. Ketelaar, "Crystal structure of the low temperature modification of ammonium bromide," Nature **134**, 250 (1934).

(11) F. Simon and C. Simpson, "Ein Umwandlungspunkt der Ammoniumsalze zwischen −30 und −40 Grad," Naturwiss. **14**, 880 (1926).

(12) J. Weigle and H. Saini, "La Structure d'Bromure D'Ammonium à Basses Temperatures," Helv. Phys. Acta **9**, 515 (1936).

(13) R. W. G. Wyckoff, "On the crystal structure of ammonium chloride," Am. J. Sci. **4**, 469 (1922).

(14) A. Smits and C. H. MacGillavry, "Die Umwandlung von festem NH_4Cl bei ungefahr −30°," Zeits. f. physik. Chemie **A166**, 97 (1933).

(15) J. H. Bruce, "The dielectric constants of ammonium salts near the lower transition temperature," Trans. Faraday Soc. **35**, 706 (1939).

(16) R. Guillien, "Sur la constante dielectrique des sels halogénés d'ammonium," Comptes rendus **208**, 1561 (1939).

(17) C. P. Smyth, "The dielectric constants of solids and molecular rotation," Chem. Rev. **19**, 329 (1936).

THE JOURNAL OF CHEMICAL PHYSICS VOLUME 12, NUMBER 3 MARCH, 1944

Potentiometric Measurements of Hydrogen Ion Concentration in Solutions of Low Dielectric Constant

ANDREW GEMANT
The Detroit Edison Company, Detroit 26, Michigan
(Received January 13, 1944)

This paper deals with potentiometric measurements of hydrogen ion concentration in solutions of *p*-toluene sulfonic acid and picric acid in xylene and dioxane. Parallel conductivity measurements complete the data. Apart from usual concentration cells, another type of cell has been tried, namely, one in which the two solutions have not only different concentrations but also different dielectric constants. The chief findings are: (1) Glass electrodes react reversibly with hydrogen ions in organic solvents of dielectric constant as low as 2.3. (2) Acids in such solvents behave essentially as weak electrolytes. (3) Deviations from the simple mass action law are explainable, to a certain extent, on the basis of varying dielectric constant with varying electrolyte concentration. (4) Hydrogen transference numbers and approximate values for absolute ionic radii can be computed from combined conductivity and e.m.f. data.

I. PURPOSE AND SCOPE OF INVESTIGATION

THE purpose of this research is to obtain, by means of e.m.f. measurements, information on the nature and behavior of electrolytic ions in liquids of low dielectric constant. Herein "low dielectric constant" is used for values in the range of 2 to 3, characteristic of dielectric liquids.

In a previous paper[1] on the same general subject, dielectric liquids containing silver and chloride ions were investigated. The lowest dielectric constant reached in that work was 2.6. As electrolytic deterioration products in oils are probably acids, it was thought useful to extend this research to cover solutions containing hydrogen ions. Also an extension of the range of dielectric constant below the value 2.6 was desirable.

The narrower aim of the present work was, therefore, to ascertain whether determinations of hydrogen ion concentration by means of e.m.f. measurements are possible in liquids of dielectric constant as low as 2.3.

The cells used in this research were acid concentration cells exhibiting liquid junction potentials. Glass electrodes were used as the reversible hydrogen electrodes. Another type of cell was investigated also, the purpose of which will be explained later in the paper. This type consists of two half-cells differing not only in the concentration of the ions, but also in the dielectric constant of the solvents. This latter difference, however, was kept small.

In addition to the e.m.f. of cells, the electrical conductivity of the solutions involved also was measured. The purpose of these determinations will also be explained later. All measurements were carried out at room temperature only.

The electrolytes used were chiefly *p*-toluene sulfonic acid and picric acid. In addition, a restricted amount of data was obtained on trichloracetic acid and hydrochloric acid. The solvents were either dioxane with small additions of water or xylene with small additions of ethyl alcohol.

II. PRINCIPLES OF INVESTIGATION

(a) The Hydrogen Ion Concentration in Dielectric Liquids

In talking of the hydrogen ion concentration $[H^+]$ in dielectric liquids, it must be realized that this term is not as accurately defined as in aqueous or alcoholic solutions. The reason is as follows: The purpose of introducing the e.m.f. method in the field of dielectric liquids is, as stated, to obtain more information on the nature of ions in them. But in order to interpret these measurements, some temporary concepts on the ions in question must be used. The procedure here, as everywhere in science, is a stepwise progression to more and more accurate definitions. For the moment the temporary concepts, used as first approximations, must suffice.

[1] Andrew Gemant, J. Chem. Phys. **10**, 723 (1942).

Thus, it is first assumed that the ion content in these solvents is so low that ionic clouds have not much significance and that the activity is identical with the concentration. Activity coefficients in the usual equations will be taken as unity. Similarly, one can simply define pH as $-\log [H^+]$, without having to decide whether it is the concentration or activity of the H^+ ions from which pH is computed.

Similarly, the effect of the ionic cloud on conductivity is assumed to be negligible. As a result of this the conductivity is used as a measure of the H^+ ion concentration. This conclusion probably will be modified in the light of future research, as it is likely that an acidic electrolyte in a dielectric does not dissociate simply into H^+ and an anion, but that complex ions (ions plus undissociated molecules) are formed in addition.[2] Complex formation is likely at higher concentrations, while at lower concentrations the simple mass action law will hold.

A further uncertainty is the value of Λ_0, the equivalent conductance at infinite dilution. This cannot be determined in the same manner as in aqueous solutions, because the degree of dissociation is very small even at lowest concentrations. For approximate numerical calculations a value around 60, valid for the sum of the two ions, can be taken as a plausible, and probably close, order of magnitude. This is justified since the value for organic ions in water is around 30, and the viscosity of solvents used in this research is near that of water.

A third uncertainty is the initial specific conductance σ_s of the solvent, which often cannot be neglected, although it is scarcely ever more than ten percent of the specific conductance of the solution. The procedure adopted in this work was always to deduct σ_s from the total conductance. In the following, σ (mhos/cm) will denote the corrected value of the specific conductance.

In using, then, the fundamental equation

$$\sigma = 10^{-3} c_i \Lambda_0, \tag{1}$$

where c_i = concentration of ion-pairs in moles per liter, and replacing c_i by $[H^+]$, we have

$$[H^+] = (10^3/\Lambda_0)\sigma. \tag{2}$$

It follows that there is proportionality between $[H^+]$ and σ. Writing 60 for Λ_0, we further have:

$$p\mathrm{H} \sim -\log \sigma - 1 \tag{3}$$

giving an approximate value of pH from the conductivity. Equation (3) is not used in the present paper.

(b) The Dissociation Constant of Acids in Dielectric Liquids

As explained above, the conductance data were used chiefly as a means for obtaining a measure of the hydrogen ion concentration, using Eq. (2). A second use of these data was for making an approximate evaluation of the dissociation constant K of the electrolytes as a function of the dielectric constant D of the solvent.

As the following shows, there is evidence that for low concentrations the simple mass action law holds. According to the latter, as applied to monovalent electrolytes,

$$c_i^2 = Kc, \tag{4}$$

where c = molar concentration per liter of the electrolyte. Combining Eqs. (1) and (4), we have

$$\sigma = (10^{-3}\Lambda_0\sqrt{K})\sqrt{c}. \tag{5}$$

The conductivity must be proportional to the square root of the electrolyte concentration if the mass action law holds. This was, indeed, the case for low concentrations. Writing, then, 60 for Λ_0, an approximate value for K is obtained.

Because of the solvent conductance σ_s it was not always possible to obtain reliable values of σ at sufficiently low concentrations. At higher values of c, on the other hand, marked deviations from Eq. (5) were noticeable, in that σ increased with a power of c higher than $\frac{1}{2}$.

The reason for such deviation is partly the formation of complex ions, as considered by Fuoss and Kraus.[2] In the present research it was observed that the dielectric constant D always increases, in some cases considerably, with the electrolyte concentration. As K increases with D, this observation accounts to a certain extent for the deviation from Eq. (5). It will be shown later that in one particular series this explanation was quantitatively satisfactory. In other cases it does not seem to account for the whole effect.

[2] R. M. Fuoss and C. Kraus, J. Am. Chem. Soc. **55**, 1019 (1933).

Apart from the question of the causes of this deviation from Eq. (5), the problem arises as to how to determine K in such cases. The data for σ evidently must be extrapolated in a reliable manner to low concentrations; from this extrapolation K can be determined.

This extrapolation was done by means of an empirical equation between σ and c. This relation, an extension of Eq. (5), valid for low *and* high values of c, was given empirically the form:

$$\sigma=(10^{-3}\Lambda_0\sqrt{K})\sqrt{c_0}(\exp{(c/c_0)^{\frac{1}{2}}}-1) \qquad (6)$$

with c_0 = a constant for a given electrolyte and solvent. It fulfills the condition that for

$$c<c_0$$

the relation degenerates into Eq. (5). The constant is obviously a measure of the concentration at which the deviation from Eq. (5) becomes noticeable. The agreement between Eq. (6) and the experimental data is usually good, so that K can be determined by it. In the experimental part it will be shown how the equation works.

(c) Hydrogen Transference Number in Dielectric Liquids

E.m.f. data obtained from concentration cells were interpreted in the following manner. With activity coefficients = 1 and room temperature, the e.m.f. E in mv is:

$$E=118(1-t_{\mathrm{H}})\log_{10}(\sigma_A/\sigma_B), \qquad (7)$$

where t_{H} = hydrogen transference number, and the indices A and B refer to the two solutions in the two half-cells. The usual procedure consisted in plotting E in mv against $\log(\sigma_A/\sigma_B)$. The points lie fairly well along a straight line across the origin. The slope of the line allows the computation of t_{H}, which is a measure of the ratio of the anion and H^+ radii (r_a and r_{H}).

Equation (7) holds, of course, for the case of identical solvents on both sides. Thus, it was used whenever pairs of solutions of the same alcohol (or water) content were combined. This procedure, however, was not always possible for solvents of low specific conductivity, say, below 10^{-12} mho/cm, because the total cell resistance became too high as compared with the grid resistance of the electrometer tube of the measuring equipment. (See Section III.)

For such solutions a new type of cell was used, as mentioned in Section I, in order to keep the total cell resistance as low as feasible. This was accomplished by filling half-cell A with a solution of relatively high D and high conductivity. This solution acted as a sort of reference solution, against which the solutions of low D and low conductivity, placed in half-cell B, were measured. This method proved useful for extending the range of D to values down to 2.3 and that of σ to values down to 10^{-13} mho/cm.

(d) Ionic Radii in Dielectric Liquids

Equation (7) has to be generalized for such cells in which both σ and the solvents are different in the two half-cells. Equation (7) is based on the change in the free energy that occurs while the ions are transferred from one concentration to another; this change in free energy is of osmotic nature. To this term a second has now to be added, accounting for the change in free energy due to the different solvation energies in the two different solvents. While an accurate calculation of this term is difficult, Born's expression[3] [see the second term of the right-hand side of Eq. (8) below] can be used as a first approximation. Born's formula for the molar solvation energy has to be applied for both cation and anion. The two terms thus obtained have to be added, and the sum multiplied by $(1-t_{\mathrm{H}})$ which is the fraction of a mole transferred across the cell accompanying the flow of a charge of 1 faraday. This will give the solvation energy in one solvent; the difference for the two solvents of dielectric constants D_A and D_B gives the change in free energy. Hence, the expression for the e.m.f. reads, for a monovalent electrolyte:

$$E=118(1-t_{\mathrm{H}})\log_{10}(\sigma_A/\sigma_B)+\frac{(1-t_{\mathrm{H}})Ne^2}{2F}\left(\frac{1}{r_{\mathrm{H}}}+\frac{1}{r_a}\right)\left(\frac{1}{D_A}-\frac{1}{D_B}\right), \qquad (8)$$

where N = Avogadro's number, e = electronic charge, $F=1$ faraday. Substituting numerical values for Ne^2/F the equation becomes

$$E=118(1-t_{\mathrm{H}})\log_{10}(\sigma_A/\sigma_B)+(1.55\times10^{-4}/b)(1-t_{\mathrm{H}})\left(\frac{1}{D_A}-\frac{1}{D_B}\right), \qquad (9)$$

[3] Samuel Glasstone, *Introduction to Electrochemistry* (D. van Nostrand Company, New York, 1942), p. 249.

where b, defined by

$$\frac{1}{b}=\frac{1}{2}\left(\frac{1}{r_{\mathrm{H}}}+\frac{1}{r_a}\right), \tag{10}$$

is an average radius in cm.

If this type of cell works according to Eq. (9) then a plot of E against log (σ_A/σ_B) should be a straight line, having a finite ordinate for the zero abscissa. The slope of the line must be 118 $(1-t_{\mathrm{H}})$, and the intercept with the ordinate axis must

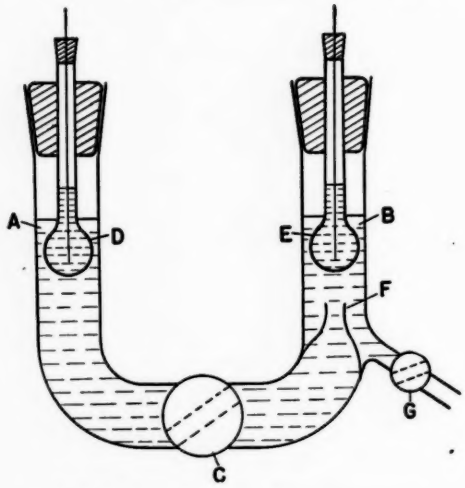

FIG. 1. Cell used for e.m.f. measurements.

increase with the term $[(1/D_A)-(1/D_B)]$. All these conditions are fairly well satisfied, as will be seen from the experimental part. From the value of the intercept b, the average radius can be computed and should—if correct—yield a value of a few angstrom units. Knowing b and t_{H}, the radii themselves are known from

$$r_{\mathrm{H}}=b/(2t_{\mathrm{H}}), \tag{11}$$

$$r_a=b/[2(1-t_{\mathrm{H}})] \tag{12}$$

but, owing to the approximate nature of Born's equation, these data for the radii can be considered only as giving the order of magnitude.

III. EXPERIMENTAL RESULTS

The e.m.f. measurements were carried out by means of glass electrodes only. No tests were made with platinum-hydrogen electrodes, as used by Harned[4] in water-dioxane mixtures of relatively high dielectric constant.

[4] H. S. Harned and C. M. Birdsall, J. Am. Chem. Soc. **65**, 54 (1943).

Figure 1 shows the cell. The two halves A and B are joined by the large-bore stopcock C. D and E are the two glass electrodes blown of "015" glass. B contains a concentric tube of smaller diameter, the continuation of A, so to speak, which opens inside B at F. B also has an outlet G. The cell stands on a suitable paraffin block inside a shielded box.*

Half-cell A and the central tube in B up to the opening F contain one of the two solutions; half-cell B contains the other. The diffusion boundary is located at F. Stopcock G is used for changing the solution in B without necessitating a change in A.

The potential difference was measured by means of a potentiometer, using an FP54 electrometer tube as null indicator.

In identical solutions the cell had a zero potential of 5 mv, which was deducted from the readings. The reproducibility of e.m.f. measurements was about ±10 percent, becoming somewhat less accurate with decreasing dielectric constant.

Conductivities were measured by means of a variable frequency power factor bridge, using an all-glass and platinum cell, constructed by J. C. Balsbaugh at M.I.T. Several frequencies in a range from 50 to 20,000 were used; these gave values for σ that were, for the most part, within a few percent of each other. This shows that the conductivity is due to free charged particles in the solution and not to dipole or polarization effects.

All preparations used in this and the following sections were chemically pure commercial products. The solvents were not purified further. The crystalline acids were dried by heating at 110° C under vacuum.

(a) *p*-Toluene Sulfonic Acid in Dioxane

Figure 2 shows the logarithm of the specific conductance in mhos/cm as a function of the logarithm of molar concentration, the circles showing measured points. The parameter of the set of curves is the dielectric constant, which was increased by the addition of small percentages of water to the dioxane. The concentration range covered was 10^{-4} to 10^{-1} mole/liter. Specific con-

* Recently a considerably improved cell has been built, to be described in another publication.

ductivities down to 10^{-13} mho/cm were obtained, and dielectric constants as low as 2.30 were investigated. Hence, the range covered includes that which is characteristic of deteriorated insulating liquids.

It can be seen, and particularly well from the curve pertaining to $D=2.85$, that the slopes approach that required by Eq. (5) for sufficiently low values of c, but that σ increases considerably more rapidly than according to Eq. (5) at higher concentrations.

The dissociation constants (approximate values) were computed by using the empirical relation (6). Its two constants, c_0 and $(10^{-3}\Lambda_0\sqrt{K})$, were chosen so as best to fit the experimental data. Figure 3 shows the kind of agreement one obtains in using this relation. The curves as shown are computed from (6), and the circles indicate experimental values. The agreement in all other cases is similar. The value of c_0 is of the order 10^{-3}, changing but little with the dielectric constant, as Table I shows.

From the factors $(10^{-3}\Lambda_0\sqrt{K})$ as used in Eq. (6) the dissociation constants were estimated by using the value 60 for Λ_0. The figures for K as a function of the dielectric constant are shown in Fig. 4. While the function appears to be a straight line for D less than 2.6, the curve bends toward the abscissa for higher values of D, a generally observed behavior.

It was mentioned in the general part that in explaining the increase of σ with c beyond the range in which the $\sqrt{c}$ relation holds, the simultaneous increase of D must be considered, as the latter in itself might account, at least partly, for the effect. In the present series (p-toluene sulfonic acid in dioxane) exactly such a situation arises. Table II refers to one set of this series, a solvent of dielectric constant 2.30, and illustrates the situation. Concentration of electrolyte, dielectric constant as measured, and corresponding values of K, as read from Fig. 4, are shown. The conductivity is then calculated from Eq. (5), using each time a different value of K. The last column gives the measured values of σ.

Figure 5 shows the result. The curve as drawn is calculated and the circles are experimental values. The increase of D more than accounts for the steep rise of σ. Similar large increases in D were observed in the other three solvents, which were of higher dielectric constant. However, it should be emphasized again that in other cases [see Section III (d)] the agreement is not as good and that other causes, such as ionic association, are also present.

The results of the e.m.f. measurements are shown in Fig. 6, the potential in mv of the cell being shown as a function of the logarithm of conductivity ratio. Data obtained from solutions of four various dielectric constants are shown on the graph. Although the points are somewhat scattered, they lie fairly well along a straight line going through the origin, as Eq. (7) requires. From the slope of the line, $t_H=0.76$ is obtained as the hydrogen transference number.

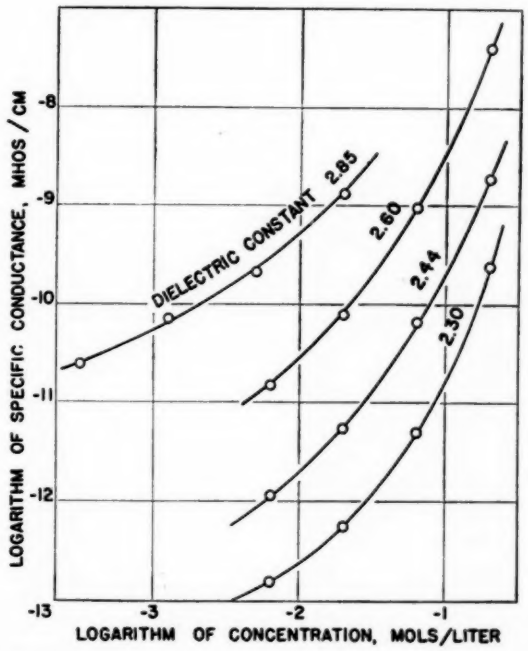

FIG. 2. Specific conductance data for solutions of p-toluene sulfonic acid in dioxane (with small additions of water).

No measurements using a special reference half-cell were carried out in this series; these will be shown in Sections III (d) and III (e).

(b) Trichloracetic Acid in Dioxane

This series will not be discussed in detail, as the lowest dielectric constant investigated was 2.6, and the results are therefore of only limited interest from our particular standpoint. Also the

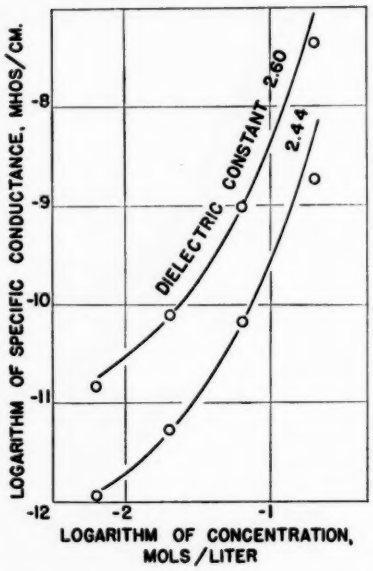

FIG. 3. Check of Eq. (6) by experimental data on σ (p-toluene sulfonic acid in dioxane).

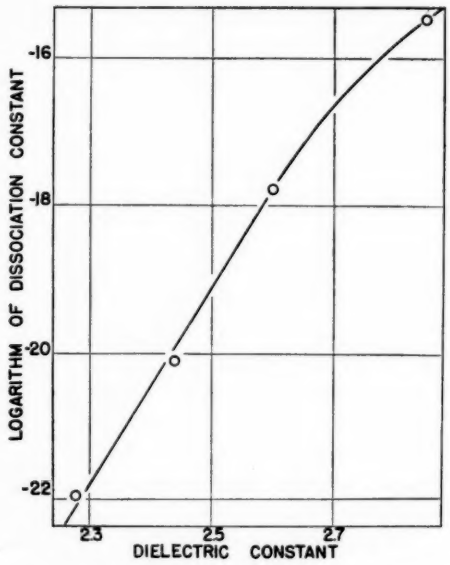

FIG. 4. Approximate dissociation constants for p-toluene sulfonic acid in dioxane.

chemical instability of the electrolyte impaired the reproducibility of the data.

Figure 7 gives a summary of the results, representing both K and t_H as functions of the dielectric constant. The average value of the latter is about 0.3, which seems rather low. If correct, it shows the hydrogen ion to become strongly solvated, as the dielectric constant decreases.

(c) Hydrochloric Acid in Dioxane

This series, too, will be presented only briefly. The lowest dielectric constant covered was 2.85, which is a relatively high value. The results are presented in Fig. 8, showing K and t_H as a function of D. The average value of t_H is 0.6. The values for K are relatively high, which is not surprising, in view of the strength of HCl in aqueous solutions.

(d) p-Toluene Sulfonic Acid in Xylene

Data now will be presented for the same electrolyte as in Section III (a), but dissolved in xylene instead of in dioxane. From the standpoint of insulating liquids, xylene, as a pure hydrocarbon, is somewhat more interesting than dioxane, which is an ether.

Figure 9 represents the conductivity data, in a manner similar to that shown in Section III (a) (Fig. 2). The validity of Eq. (5) at low concentrations is evident from the slopes. For the calculation of K Eq. (6) was again used. Table III shows the constant c_0 as a function of D. It will be noted that c_0 decreases with decreasing dielectric constant. The deviation from the simple mass action law begins at lower concentrations the lower the dielectric constant.

The variation of K with the dielectric constant is shown in Fig. 10. In spite of the considerable difference of the solvents, the curves in Fig. 4 and Fig. 10 are very similar, K appearing somewhat larger in xylene than in dioxane. The solubility of the electrolyte in the pure solvents, however, is considerably higher for dioxane than for xylene. In the case of the latter there were no measurements at all possible without the addition of ethyl alcohol.

The present series offers an example in which the large increase of σ with c cannot be explained solely on the basis of an increased dielectric constant. Table IV, in analogy to Table II,

TABLE I.

D	c_0
2.30	2.5×10^{-3}
2.44	2.0
2.60	2.0
2.85	1.7

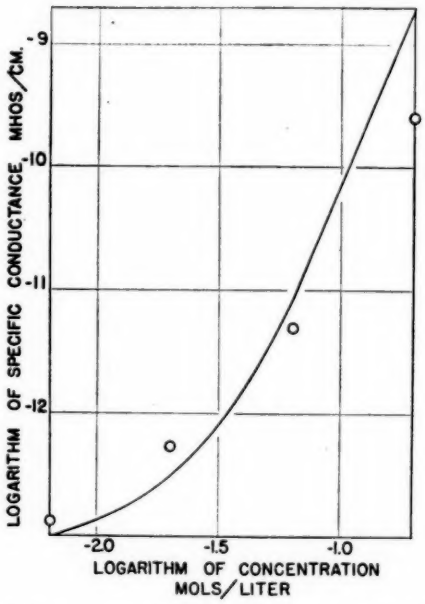

FIG. 5. Experimental σ *vs.* c relation, explained by the simultaneous increase of D (p-toluene sulfonic acid in dioxane).

shows a computation carried out for solvent $D=2.40$. It can be seen that the increase of D (and K) with the concentration is not large enough to account fully for the steep σ *vs.* c curve. But even in such cases the increase of D must be considered before any other theory is applied.

The e.m.f. measurements are summarized in Fig. 11. Equation (7) is fairly well fulfilled and the hydrogen ion transference number, as computed from the slope, is $t_H=0.80$.

Measurements with solvent $D=2.40$ were not feasible, and therefore a reference solution of relatively high conductance was used, as explained in the general part. Figure 12 shows the result of these measurements. The plus sign on the potential scale indicates half-cell A (the reference cell) as the positive pole. The solution in half-cell B had dielectric constants 2.40, 2.47,

TABLE II.

c	D	K	σ (calc.)	σ (measured)
0.0000	2.30	—	—	—
0.0064	2.35	4.0×10^{-22}	1.0×10^{-13}	1.5×10^{-13}
0.020	2.38	1.2×10^{-21}	3.0×10^{-13}	5.5×10^{-13}
0.064	2.54	3.1×10^{-19}	8.5×10^{-12}	4.9×10^{-12}
0.20	3.05	5.0×10^{-15}	1.8×10^{-9}	2.4×10^{-10}

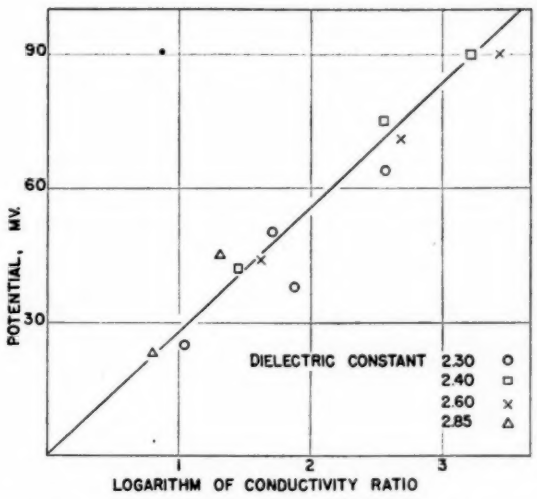

FIG. 6. E.m.f. data for p-toluene sulfonic acid in dioxane.

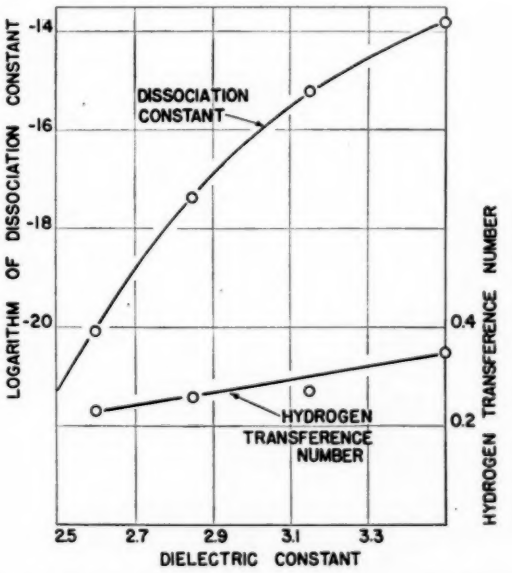

FIG. 7. Dissociation constant and hydrogen transference number data for trichloracetic acid in dioxane.

and 2.52, as shown on the graph. Two different reference solutions were used in half-cell A, one of $D=2.67$ and $\sigma\sim10^{-9}$ mho/cm, and another of $D=2.52$ and $\sigma\sim10^{-10}$ mho/cm. The first, having the higher conductivity, appeared more reliable for the purpose. A small percentage of carbon tetrachloride was added to these two solutions in order to increase their density and minimize mixing at the boundary F (see Fig. 1) during measurements. The points marked by ○ and + in Fig. 12 refer to cells with reference solution

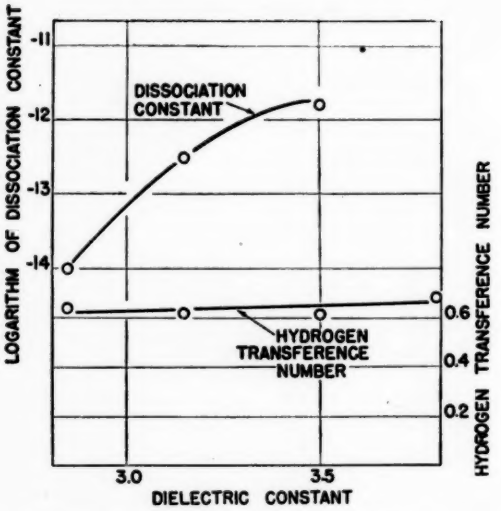

FIG. 8. Dissociation constant and hydrogen transference number data for hydrochloric acid in dioxane.

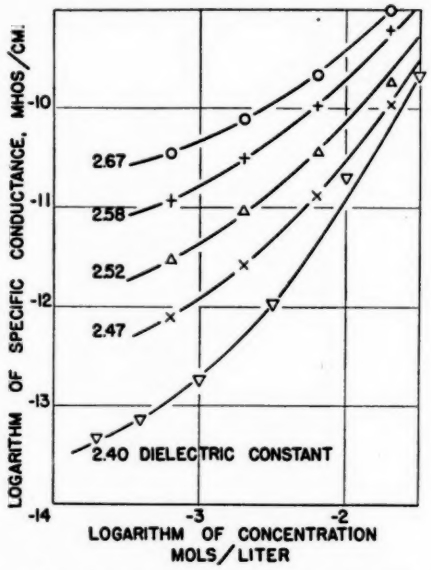

FIG. 9. Specific conductance data for solutions of *p*-toluene sulfonic acid in xylene (with small addition of ethyl alcohol).

$D=2.67$; those marked by × and △ refer to a reference solution $D=2.52$.

An equation of the type of (8) is well fulfilled by the experimental data. The slope of the straight lines is the same as that of Fig. 11, as required, the only deviation being shown by solutions $D=2.40$ of very low conductance. The intercepts with the ordinate axis are negative, as required by the term $(1/D_A-1/D_B)$. Selecting the two intercepts referring to the reference solution $D=2.67$, and plotting them *vs.* $(1/D_A-1/D_B)$ as in Fig. 13, an approximate slope (dotted line) was obtained that may be interpreted as the factor of the second term in Eq. (9). This would give for the average ionic radius (b) 1.7A units. Using this value and $t_H=0.80$ in Eqs. (11) and (12) the values of the individual ionic radii are found to be $r_H=1$A and $r_a=4$A. While r_H appears rather low, r_a is of the right order for a strongly solvated ion. Ions in insulating oils are probably even larger.[5]

(e) Picric Acid in Xylene

The third series to be given in detail refers to picric acid solutions in xylene. While the solvent is a pure hydrocarbon in this case, the solubility of the electrolyte is quite appreciable, which adds to the interest in this combination.

Figure 14 presents the results of conductivity

[5] Andrew Gemant, Phys. Rev. **58**, 904 (1940).

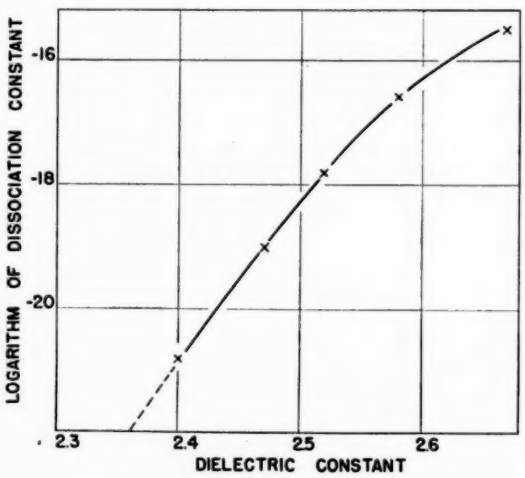

FIG. 10. Approximate dissociation constants for *p*-toluene sulfonic acid in xylene.

vs. concentration. The lowest dielectric constant is 2.35. The slope of the lines follows very nearly that required by Eq. (5). Since the dielectric

TABLE III.

D	c_0
2.40	0.46×10^{-3}
2.47	0.53
2.52	0.92
2.58	1.2
2.67	2.2

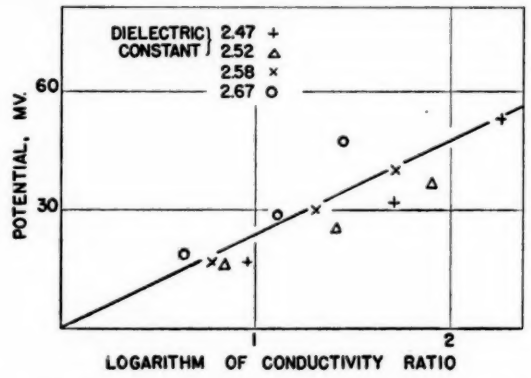

FIG. 11. E.m.f. data for *p*-toluene sulfonic acid in xylene.

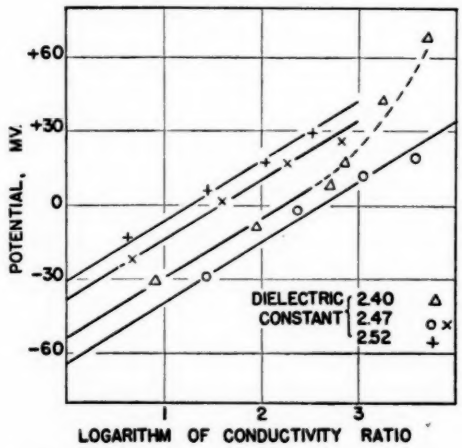

FIG. 12. E.m.f. data obtained with reference solution of high σ in one half-cell (*p*-toluene sulfonic acid in xylene).

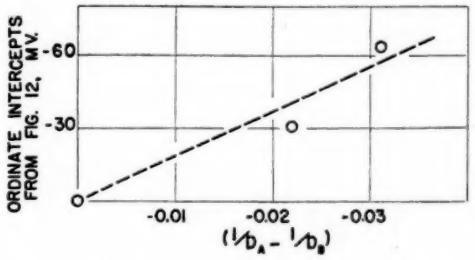

FIG. 13. Plot of intercepts with ordinate axis from Fig. 12 (*p*-toluene sulfonic acid in xylene).

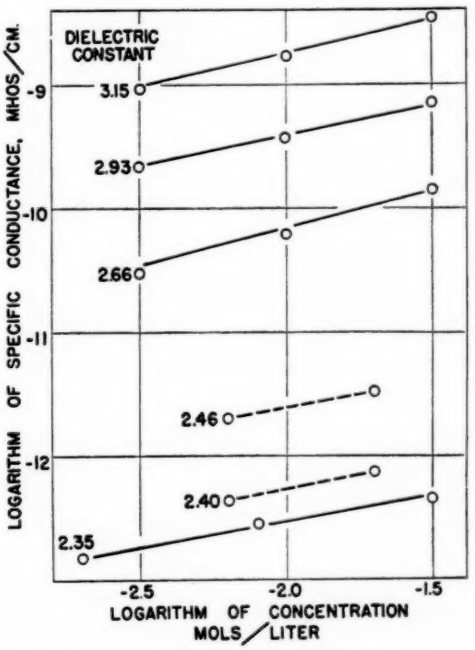

FIG. 14. Specific conductance data for picric acid in xylene (with small additions of ethyl alcohol).

constant, as measured, changes very little, the agreement with Eq. (5) is to be expected. For the solvent $D=2.35$, for example, the highest value measured was 2.39. The dissociation constants, accordingly, were calculated from Eq. (5) in this case; the result is shown in Fig. 15.

The curve agrees very closely with that in Fig. 10, even as to numerical values, although the two electrolytes are chemically different (a sulfonic acid in one case and a nitrophenol in the other). This also shows that non-specific electrostatic effects dominate in determining the degree of dissociation.

TABLE IV.

c	D	K	σ (calc.)	σ (measured)
0.0000	2.40	—	—	—
0.0010	2.40	1.5×10^{-21}	7.0×10^{-14}	1.9×10^{-13}
0.0032	2.40	1.5×10^{-21}	1.3×10^{-13}	1.1×10^{-12}
0.010	2.42	4.5×10^{-21}	4.0×10^{-13}	1.6×10^{-11}
0.032	2.46	5.0×10^{-20}	2.4×10^{-12}	2.5×10^{-10}

E.m.f. measurements are presented in Fig. 16. They show results obtained from cells containing a reference solution in half-cell *A*. This solution had a dielectric constant of 3.15 and $\sigma\sim10^{-9}$ mho/cm. The dielectric constants of the solutions of half-cell *B* are shown on the graph.

The three curves at the left side of the graph behave as required by Eq. (9). The computations based on them will be discussed presently. With further decrease of D the curves show a trend that is only qualitatively in keeping with the theory. Quantitatively they indicate a consider-

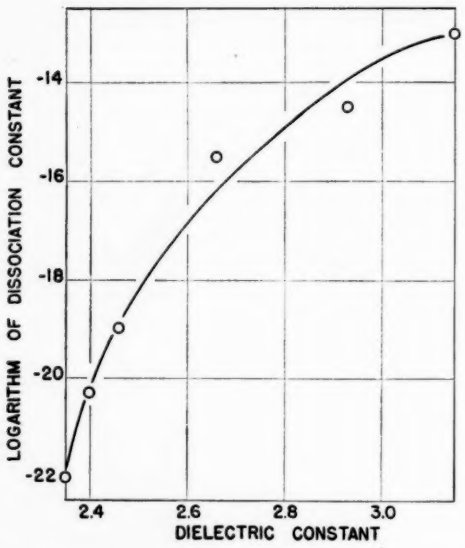

FIG. 15. Approximate dissociation constants for picric acid in xylene.

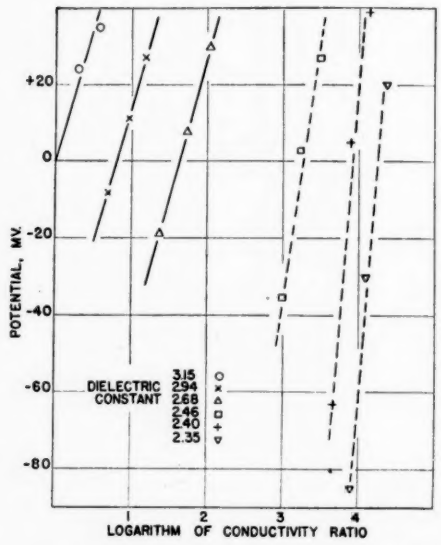

FIG. 16. E.m.f. data obtained with reference solution of high σ in one half-cell (picric acid in xylene).

able divergence from Eq. (9). The slopes are steeper than expected, and the intercepts with the ordinate become excessively large. It is not possible to state definitely whether the simple Eq. (9) breaks down in this range, or whether the data are not quite reliable because the glass electrode ceases functioning reversibly with these solutions. The lines were drawn dotted because

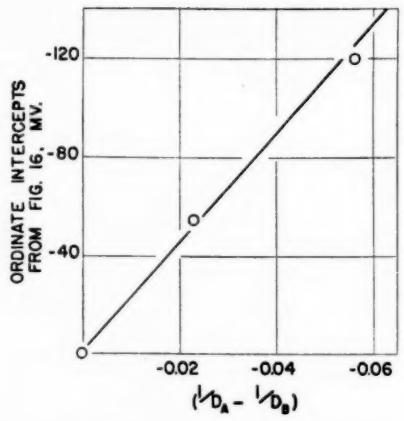

FIG. 17. Plot of intercepts with ordinate axis from Fig. 16 (picric acid in xylene).

of this uncertainty. However, it is worth noting that there is a pronounced change of the potential with varying hydrogen ion concentration. This fact will have to be remembered when attempts are made to utilize the knowledge obtained in this work for testing insulating oils for their hydrogen ion concentration. Continuation of the present work along these lines is now planned; such work would tie up with the research of J. D. Piper and collaborators on insulating liquids.[6]

From the slopes of the three curves at the left side the value of t_H is found by calculation to be 0.40.

The intercepts with the ordinate axis are plotted against $(1/D_A - 1/D_B)$ in Fig. 17. Using Eq. (9), $b = 4.2$A is computed from the slope; this is the average radius. The individual radii from Eqs. (11) and (12) become $r_H = 5$A and $r_a = 3$A. These are of the expected order of magnitude for the size of strongly solvated ions. [The term "solvated" may be an expression either for general dipolar orientation, or for the formation of complex molecules (ion plus solvent molecules) having characteristic absorption spectra.[7]]

The author wishes to thank his colleagues Howard Boltz, A. G. Fleiger, and N. A. Kerstein for valuable cooperation in this research.

[6] J. D. Piper, A. G. Fleiger, C. C. Smith, and N. A. Kerstein, Ind. Eng. Chem. **34**, 1505 (1942).

[7] R. W. Gurney, *Ions in Solution* (Cambridge University Press, 1936), p. 24.

THE JOURNAL OF CHEMICAL PHYSICS VOLUME 12, NUMBER 3 MARCH, 1944

The Principles of Thermodynamics

BORIS LEAF
Noyes Chemistry Laboratory, University of Illinois, Urbana, Illinois
(Received November 24, 1943)

A formulation of thermodynamics has been developed which points out the restrictions of classical treatments. This formulation in terms of potential and charge concepts predicts the property ascribed to the entropy of increasing during thermodynamic processes and leads to an equation for entropy produced and heat dissipated in irreversible processes. The postulates of the treatment presented have allowed deduction of a generalized form of the second law of thermodynamics which applies to each energy field of the system. These concepts have been further developed in discussion of the phase rule; the functions H, A, and F; a generalization of Kelvin's postulate; and a generalization of the Carnot cycle. The results obtained have permitted derivation of the principles of Brønsted's system of energetics.

IT is the purpose of this paper to investigate the basic assumptions of thermodynamics. The classical formulation of thermodynamics involves concepts which greatly restrict its generality. We shall attempt to develop a formulation of thermodynamics within the classical framework in such a way as to demonstrate the limitations of the classical treatment and possibly to indicate the approach to a more general treatment. Our results will enable us to derive the principles of energetics as enunciated by Brønsted[1] so that these principles will appear as special results of thermodynamics.

One of the first considerations in the classical treatment of thermodynamics is the definition of the system and the state of the system. The concept of the state of the system imposes serious limitations on the applicability of the results of the classical treatment. A thermodynamic system may be any portion of the universe we care to consider. The properties of a system are considered to be functions of a certain few variables, which are generally chosen to be the temperature, entropy, pressure, volume, composition, etc. When these functions are defined in the system, a set of values for these variables is said to describe a state of the system. Thermodynamic processes consist of the passage of the system from one state to another. The limitation imposed by this formulation is at once apparent; we are unable to treat the system when it is not in a defined state. This immediately precludes the possibility of treating flowing systems, problems of diffusion, viscosity, or heat conduction, since in none of these instances do the systems considered have well-defined functions such as the pressure or temperature. Only when the system is static can we define such functions. Consequently, formulated according to the concept of the state of the system, thermodynamics is not designed to give information about flowing, non-static systems, or systems in the process of transition between initial and final states of a process.

It appears that in order to overcome the restrictions imposed by the classical treatment one must replace the concept of the state by something more general. This entails description of the region under consideration by means of differential equations giving the variation with time of the properties at each point in the various energy fields of the region. Such a method is illustrated in an article by Meixner.[2] Since, however, in this paper we desire to remain within the classical framework we will employ the concept of the state. We note that if we are content to consider only problems concerned with changes of a system between initial and final states the classical treatment is adequate.

Let us now consider a certain system which we will suppose to exist in a certain state. The intensity of energy is specified by the potential functions corresponding to the various forms in which energy may be manifest in the system, e.g., the temperature T, pressure P, chemical potential μ_i, etc. Corresponding to each potential

[1] J. N. Brønsted, Phil. Mag. [7] **29**, 449 (1940); J. Phys. Chem. **44**, 699 (1940).

[2] J. Meixner, Ann. d. Physik **39**, 333 (1941).

function for the system there exists an energy charge function, as for example, the entropy S corresponding to the temperature, the volume V corresponding to the pressure, the mass m_i of the ith chemical component corresponding to the chemical potential of component i. When a quantity of energy charge enters a system against the prevailing potential values, the energy of the system increases. The increase in energy of each homogeneous portion or phase of a system, characterized by a single value of each potential function, is given by the sum of the increases in energy in the various forms in which it may enter that phase. As the defining equation for the increase of energy of a phase during an infinitesimal change of state we write

$$dE = TdS - PdV + \sum \mu_i dm_i + \cdots. \quad (1)$$

The increase in energy of the whole system is the sum of the increases in the homogeneous portions. If the system is a single homogeneous phase its energy increase is given by (1).

About the system there exist homogeneous surroundings for which the increase of energy is given by

$$dE' = T'dS' - P'dV' + \sum \mu_i' dm_i' + \cdots. \quad (2)$$

It has been pointed out[3] that in an actual instance, if a finite system at a certain set of potential levels is in contact with surroundings at a different set of levels then neither Eq. (1) nor Eq. (2) describes the detailed process that occurs. Local inhomogeneities will develop, first, at the boundary between system and surroundings and then these disturbances will spread throughout the system; finally, the disturbances will become uniformly distributed and the system is again homogeneous. As soon as the local inhomogeneities appear, however, the system is no longer in a thermodynamic state and cannot be treated in the classical manner. In order to treat the problem the method is to replace the actual path, traversed by the system in passing from initial to final states, by an idealized path in which a state is defined for the system at every point. Since classically we are interested only in the end states, such a method gives the correct result and the treatment is much simpler than that required in a detailed description of the actual process. Equations (1) and (2) are therefore valid within the limits of utility of the classical treatment since they are equations defining energy changes along the idealized path.

There is an alternative method of viewing the limitations of Eqs. (1) and (2). The local inhomogeneities attend the transfer of energy charges between system and surroundings. If the rate of distribution of these charges throughout the system is rapid compared to our experimental observation of the system, the system will at every stage of the process appear homogeneous. Consequently, by being sufficiently slow in our measurements as to allow disappearance of the local disturbances we will find the changes of state of the system and surroundings to be described by Eqs. (1) and (2).

The range of validity of Eqs. (1) and (2) coincides with the range of applicability of the classical method using the state concept. To get a more detailed description of the process as a function of time one must resort to a more general method such as the use of differential equations for the various energy fields as indicated earlier.

Having defined the energy changes in the system and surroundings we can now formulate the law of conservation of energy. The composite system consisting of the system and its surroundings is isolated with respect to all forms of energy. The region designated as the surroundings during a process involving the system is always chosen large enough so that the composite system satisfies this condition. Since the total energy is conserved for the composite system

$$dE + dE' = 0. \quad (3)$$

In consideration of energy exchanges between system and surroundings it is necessary to distinguish between charge entering the system from the surroundings and increase in charge in the system resulting from processes within the system. If K is the charge corresponding to a particular form of energy, then δK, the charge entering the system, is equal to $-dK'$, the charge leaving the surroundings

$$\delta K = -dK'. \quad (4)$$

[3] F. H. MacDougall, private communication.

The total gain in charge of the system is written as dK and is the sum of the quantity δK entering from the surroundings and the charge produced in the system, during an infinitesimal process. For the surroundings no distinction is made between dK' and $\delta K'$. The surroundings may be imagined to be infinite reservoirs of the various forms of energy each at a certain potential level. It is only in the system that changes of energy involving charge production occur.

We can now demonstrate that the total charge function in the total energy field of a system must increase in the system and its surroundings. Let us consider a field of energy which we will designate as a ϕ-Z field. We shall assume that this field is conservative. This ϕ-Z field satisfies two conditions, namely:

(a) The total ϕ-Z energy in the system and the surroundings is conserved.

$$\phi dZ+\phi' dZ'=0 \tag{5}$$

or

$$\phi dZ-\phi'\delta Z=0. \tag{6}$$

(b) The gradient of the potential function ϕ determines the total force field on an element of charge δZ as it passes between system and surroundings and therefore determines the direction of flow of δZ.

$$(\phi-\phi')\delta Z=(\phi'-\phi)dZ'\leqq 0. \tag{7}$$

According to relation (7) if

$\phi>\phi'$, then $\delta Z<0$ and Z leaves the system.
$\phi<\phi'$, then $\delta Z>0$ and Z enters the system.

From (6)

$$(\phi-\phi')\delta Z+\phi(dZ-\delta Z)=0.$$

Hence

$$\phi(dZ-\delta Z)=-(\phi-\phi')\delta Z\geqq 0 \tag{8}$$

$$dZ\geqq\delta Z. \tag{9}$$

This interesting result shows that $dZ+dZ'\geqq 0$ so that the charge in the ϕ-Z field must increase or reach a maximum in the system and its surroundings. If we suppose that the total energy field can be identified with the ϕ-Z field so that it satisfies relations (5) and (7) then we are led to expect the existence of a charge function with the property of always increasing. This property, of course, is associated with the entropy, so that we anticipate one of the most important properties of the entropy.

The condition for equilibrium between system and surroundings is

$$\phi=\phi' \tag{10}$$

so that

$$dZ=\delta Z. \tag{11}$$

The identification of the total energy field with the ϕ-Z field which obeys relations (5) and (7) is permissible within the classical treatment based on the idea of the state of the system. In this treatment charges simply move from one potential level to another. Kinetic energy is excluded from consideration since a system with moving parts is not in a thermodynamic state. The entire energy field is therefore of the potential energy type for which there exists the potential function ϕ whose gradient determines the direction of motion of the total energy charge δZ. This charge is the sum of the charges for the individual component fields. For example, if the total field consists of thermal and electrical fields, the charge δZ is the sum of a certain number of entropy units and a certain number of electrical charge units. Corresponding to this composite charge the potential ϕ is a thermoelectric potential function.

Since we identify the total energy field with the ϕ-Z field

$$dE=\phi dZ. \tag{12}$$

We now suppose that the total energy field can be divided into two fields one of which is a T-S or thermal field for which

$$dS\geqq\delta S \tag{13}$$

and the other of which is a ψ-Y or work field for which

$$dY=\delta Y. \tag{14}$$

Since $dZ=dS+dY$ this is consistent with (9). At equilibrium, therefore, according to (11)

$$dS=\delta S. \tag{15}$$

In subdividing the field we let

$$dE=\phi dZ=TdS+\psi dY \tag{16}$$

so that we see by comparison with Eq. (1) that

$$\psi dY=-PdV+\sum\mu_i dm_i+\cdots. \tag{17}$$

The ψ-Y field is really the aggregate of all the individual fields except the thermal field which we have singled out for special consideration here.

We can now obtain a very important relation giving the entropy produced during irreversible processes. From (6) and (14) we find

$$TdS - T'\delta S + (\psi - \psi')dY = 0. \quad (18)$$

This equation can be written, according to (13), as

$$T(dS - \delta S) = -(T - T')\delta S - (\psi - \psi')dY \geqq 0. \quad (19)$$

Relation (19) is of fundamental importance. It can also be written

$$T(dS + dS') = (T - T')dS' + (\psi - \psi')dY' \geqq 0. \quad (20)$$

The term $T(dS+dS')$ is an energy dissipation function representing energy of internal processes in the system. It represents energy converted into heat in the process of transferring charges dS' and dY' from potential levels T' and ψ' to T and ψ. Meixner[2] has related this dissipation function to the energy of diffusion, heat flow, and viscosity in the system during irreversible processes. As we shall see, this term has the properties of Brønsted's "energetic heat evolution."[1]

Now we notice that the transfer of thermal charge δS and the transfer of work charge dY between system and surroundings are independent processes. Consequently from (19) we find an inequality on each of the two fields.

$$(T - T')\delta S \leqq 0 \quad (21)$$

$$(\psi - \psi')dY \leqq 0. \quad (22)$$

Relation (22) substituted into (18) shows that

$$TdS - T'\delta S \geqq 0 \quad (23)$$

a relationship which, as we shall see, reduces to the ordinary statement of the second law of thermodynamics. At equilibrium, when, according to (15), $dS = \delta S$, we find from (19) that

$$T = T' \quad \text{and} \quad \psi = \psi'. \quad (24)$$

We define a reversible process between system and surroundings as one in which there are only infinitesimal differences between the potentials of the system and those of the surroundings. At any stage in the process, equilibrium conditions prevail between system and surroundings so that $dS = \delta S$. Such processes, of course, take an infinite time. Notice that our use of the term equilibrium is in a different sense from its use in statements such as "Supercooled water is not at equilibrium." This statement is concerned with the stability of one state of the system as compared to another possible state. We allow the possibility of supercooling water reversibly with equilibrium prevailing between system and surroundings. It is only necessary that the temperatures (and other potentials) of the system and surroundings be in balance throughout the process. For any reversible processes the dissipation function is zero. The magnitude of the dissipation function is the criterion of the degree of irreversibility of a process.

According to (22) a directional condition governs the motion of dY between system and surroundings. Charge moves from higher to lower potential. This is similar to the condition in relation (7) for the motion of δZ in a conservative ϕ-Z field. However, ψ-Y energy is not conserved except for $\psi = \psi'$ or for $dY = 0$, when the equality holds in (22), so that

$$\psi dY + \psi' dY' = 0.$$

If this equation were true for $\psi \neq \psi'$ and $dY \neq 0$, it would follow from (22) that $dY > \delta Y$ which contradicts our assumption (14). Except when $\psi = \psi'$ or $dY = 0$ it is necessary to combine thermal energy with work energy to make a conservative energy field.

For thermal energy likewise, according to (21), a directional condition governs motion of entropy between system and surroundings. Entropy moves from higher to lower potential. From (20) we see that when $\psi = \psi'$ or $dY = 0$, the thermal energy is also conserved.

$$TdS + T'dS' = 0.$$

If we restrict the changes in the ψ-Y field to P-V changes only, then, according to (17), $dY = 0$ implies constant volume and $\psi = \psi'$ implies equality of pressure between system and surroundings. These are the conditions for constant volume and constant pressure (i.e., $P = P' =$ constant) calorimetry, respectively, so that in ordinary calorimetric processes the thermal energy and work energy are individually conserved.

Let us now define two terms which will enable us to present the ordinary statements of the first and second laws of thermodynamics as results of our previous discussion. Define

$$dq = -T'dS' \quad \text{or} \quad dq = T'\delta S \qquad (25)$$
$$dw = \psi' dY' \quad \text{or} \quad dw = -\psi' dY.$$

dq is the heat entering the system from the surroundings and dw is the work done upon the surroundings. From (16) and (18) we find

$$dE = T'\delta S + \psi' dY \qquad (26)$$

and therefore

$$dE = dq - dw \qquad (27)$$

which is the usual formulation of the first law of thermodynamics. From (23) and (22) we find

$$dq \leqq TdS \qquad (28)$$

$$dw \leqq -\psi dY. \qquad (29)$$

Relations (28) and (29) are the usual expressions of the second law of thermodynamics. Each implies the other because of (18) which can be written

$$TdS - dq = -\psi dY - dw \geqq 0.$$

At this point we have divided the total energy field into two parts. ψ-Y energy has been given the generic name of work energy to distinguish it from T-S or thermal energy. In the absence of other work terms it reduces to pressure-volume work. However, it is often necessary to subdivide the ψ-Y energy into several component fields as shown in Eq. (17). Let us designate as π-K fields the component fields of the ψ-Y work field. From (14)

$$\sum dK = \sum \delta K \qquad (30)$$

and from (22)

$$\sum (\pi dK - \pi' \delta K) \leqq 0, \qquad (31)$$

the summation being over all the component π-K fields. Define

$$dg = \pi' dK' = -\pi' \delta K \qquad (32)$$

so that

$$dw = \sum dg = -\sum \pi' \delta K. \qquad (33)$$

Examples of various types of π-K energy are:

π	K	dK	dg	Type of Energy
P	V	$-dV$	$P'\delta V$	Pressure-volume
μ_i	m_i	dm_i	$-\mu_i'\delta m_i$	Chemical
$\mathcal{E}$	ϵ	$d\epsilon$	$-\mathcal{E}'\delta\epsilon$	Electrical.

It may often be true that $dK = \delta K$ as in the case where K represents the volume V. We shall assume

$$dV = \delta V \qquad (34)$$

so that for P-V work

$$dg = P' dV. \qquad (35)$$

Also, in the absence of chemical reactions in the system

$$dm_i = \delta m_i.$$

However, if reactions occur, dm_i, the gain in mass of substance i in the system, may be different from δm_i, the mass entering from the surroundings. But in either case

$$\sum dm = \sum \delta m_i \qquad (36)$$

since in all ordinary processes mass is conserved. We readily see from this discussion that the logical unit of charge for chemical energy is the unit of mass. It is a widespread custom among chemists to take the mole as the unit of charge so that μ_i is a partial molal quantity rather than a partial mass-unit quantity. For many purposes this is satisfactory and advantageous. But if we replace m_i by n_i, the number of moles of substance i, none of Eqs. (14), (30), or (36) will hold.

Now if we write (31) in the form

$$\sum \pi (dK - \delta K) + \sum (\pi - \pi')\delta K \leqq 0$$

we see that

$$\sum \pi (dK - \delta K) \leqq 0 \qquad (37)$$

and

$$(\pi - \pi')\delta K \leqq 0 \quad \text{or} \quad dg \leqq -\pi \delta K. \qquad (38)$$

Relation (38) gives a directional condition governing motion of δK between system and surroundings. At equilibrium the equality holds in (37) and $\pi = \pi'$ in (38).

When $dK = \delta K$ for any of the π-K fields we find from (38) that

$$(\pi - \pi')dK \leqq 0 \quad \text{or} \quad dg \leqq -\pi dK. \qquad (39)$$

Such a π-K field is independent of the other fields. The increase in charge results only from charge entering from the surroundings; none is formed within the system at the expense of the charge functions of the other π-K fields. The number of independent π-K fields in the total work field is the number of π-K fields for which

$dK = \delta K$. In the case of chemical fields this number is known as the number of "components" of the system. Relation (39) is a generalization to the individual π-K fields of the second law of thermodynamics given in (29). It is true only for those fields *for which* $dK = \delta K$ (as, for example, in the cases where K represents V or $\sum m_i$).

From this point on, whenever we refer to a π-K field we shall mean one for which $dK = \delta K$ so that relation (39) will apply.

We have now concluded the discussion of the principles of thermodynamics. The remainder of the paper will be concerned with application and development of the concepts already presented. Let us summarize the important postulates on which our formulation of thermodynamics is based.

1. A system is defined by its energy fields, each of which is characterized by a potential function and a charge function. This is the assumption which limits classical thermodynamics to treatment of systems in "states."

2. Energy is conserved according to Eqs. (3) or (5).

3. The total energy field is conservative in the sense of relation (7); i.e., there exists a potential function whose gradient regulates motion of the total charge function.

4. The total energy field can be subdivided into a thermal field and work fields, the thermal field having the property that $dS \geqq \delta S$ and the work fields having the property that $dK = \delta K$.

Postulate (2) is, of course, equivalent to the first law of thermodynamics; postulates (3) and (4) imply the usual statement of the second law but also allow formulation of the important relation (19) for the dissipation function.

It was suggested by the reviewer of this article that reference be made to the formulation of thermodynamics presented by C. Caratheodory[4] and by M. Born.[5] These authors have shown that for reversible processes dq has the form of a Pfaff differential expression. A consequence of their statement of the second law (Caratheodory's principle) is that for reversible processes dq has an integrating factor which can be defined as the temperature T and that the resulting exact differential dq/T defines the entropy. By this approach the authors are able to relate some problems of thermodynamics to the mathematical structure built around the Pfaff expressions. This development of the subject appears to have certain deficiences:

1. It is not readily extended to give information about irreversible processes. For such processes, of course, dq does not have the form of a Pfaff expression. The important result in relation (19) for the energy dissipation, which clarifies the nature of irreversible processes, is not obtainable since the distinction between heat entering the system from the surroundings and the heat generated within the system is not made.

2. There is undue emphasis on the unique properties of heat. There seems to be little more reason to introduce the temperature as an integrating factor for the heat than to define the pressure, for example, as an integrating factor for pressure-volume work. We have, in this paper, introduced T and S on an equal basis with the other potentials and charges of the system.

THE PHASE RULE

If we consider a system whose energy is divided among T-S, P-V, and chemical energy fields, the number of chemical "components" C is one less than the number of π-K fields, the remaining π-K field being, of course, the P-V energy. C is the number of chemical fields for which we can write $dK = \delta K$. The total number of fields is therefore $C+2$. If the total energy of this system is specified, the energy of $C+1$ fields can be varied arbitrarily. The distribution of energy among the various fields determines the properties of the system. All the "intensive" properties of the system are determined when $C+1$ variables are fixed.

Our considerations so far have dealt with a homogeneous system characterized by a single value for each independent variable throughout. Consider now a system which is not necessarily a single phase but which may have different values for the potential functions within its boundaries. Assume there are p homogeneous phases in the system and that the system is so isolated that no form of energy is exchanged with the surroundings.

$$\sum_p T_p dS_p \geqq 0, \quad \sum_p \pi_p dK_p \leqq 0. \tag{40}$$

[4] C. Caratheodory, Math. Ann. **67**, 355 (1909).
[5] M. Born, Physik. Zeits. **22**, 218, 249, 282 (1921).

At equilibrium

$$\sum_p T_p dS_p = 0, \quad \sum_p \pi_p dK_p = 0, \tag{41}$$

and

$$\sum_p dS_p = 0, \quad \sum_p dK_p = 0. \tag{42}$$

Hence at equilibrium T and π are uniform throughout the system. Each form of energy is at one potential level in an isolated system at equilibrium.

Even though the system is not isolated the potentials must nevertheless be uniform throughout. This follows from the fact that the composite system formed of the system and its surroundings is itself completely isolated so that at equilibrium the potentials are uniform throughout the composite system. But the system considered is a part of the composite system and therefore at equilibrium it must be at constant potential.

This result enables us very simply to derive the phase rule. The number of independent variables in p separate phases is $p(C+1)$. If these phases are parts of a system at equilibrium they must all be at the same potentials, a condition which imposes $(C+2)(p-1)$ relationships on these variables. The number of independent variables remaining for the system is

$$f = p(C+1) - (C+2)(p-1) = C - p + 2. \tag{43}$$

DERIVED FUNCTIONS

As a result of our previous discussion certain facts about the derived functions H, A, and F are clearly brought out. Define

$$H = E + PV \tag{44}$$

$$A = E - TS \tag{45}$$

$$F = H - TS. \tag{46}$$

According to the first law and Eqs. (33) and (35)

$$dE = dq - dw = dq - P'dV - dw^*, \tag{47}$$

$$dE \leqq TdS - dw = TdS - P'dV - dw^*, \tag{48}$$

where dw^* includes all the work done on the surroundings other than P-V work. If the system undergoes a change at constant volume with $dw^* = 0$, then $dE = dq$.

$$dH = dq - P'dV - dw^* + PdV + VdP \tag{49}$$

$$dH \leqq TdS - P'dV - dw^* + PdV + VdP. \tag{50}$$

If the pressure of the system P equals the pressure of the surroundings P' and is constant, and if furthermore $dw^* = 0$, then $dH = dq$. The increase in enthalpy equals the heat of reaction for the type of reaction carried out in an open vessel so that the pressure of the reaction mixture is always atmospheric pressure and no work other than pressure-volume work against the atmosphere is performed.

$$dA \leqq -SdT - dw. \tag{51}$$

At constant temperature

$$-dA \geqq dw. \tag{52}$$

The increase in work function for a system in an isothermal process is the negative of the maximum work of the process. In an isothermal process for which $dw = 0$

$$-dA \geqq 0. \tag{53}$$

Therefore, at equilibrium in a system at constant temperature which can do no work against the surroundings, $dA = 0$ and A is a minimum.

$$dF \leqq -SdT - P'dV - dw^* + PdV + VdP. \tag{54}$$

If the temperature of the system is constant and if the pressure of the system P equals that of the surroundings P' and is constant then

$$-dF \geqq dw^*. \tag{55}$$

If we use the term "available work" to describe dw^*, then the increase in free energy of a system in an isothermal process such that the pressures of the system and surroundings are equal and constant is equal to the negative of the maximum available work. If $dw^* = 0$ in such a process then

$$-dF \geqq 0. \tag{56}$$

Therefore, at equilibrium in a system at constant temperature and pressure (where $P = P'$) which can do no work other than pressure-volume work against the surroundings, $dF = 0$ and F is a minimum.

GENERALIZATION OF KELVIN'S POSTULATE

We shall now investigate certain consequences of our generalized statement of the second law as given in relation (39).

Let a system operate through a cycle.

$$\oint dS = \oint dq_{max}/T = 0.$$

If the cycle is performed at constant temperature

$$\oint dq_{max} = 0.$$

Hence, for any isothermal cycle

$$q = \oint dq \leqq \oint dq_{max} = 0.$$

Since $\Delta E = 0$ for the cycle

$$w = q \leqq 0.$$

Both w and q must be negative or zero. Heat cannot flow into the system and serve as a source of energy to do work upon the surroundings in an isothermal cycle. This statement of the second law is known as the Kelvin postulate.

Similarly during the cycle

$$\oint dK = \oint -dg_{max}/\pi = 0.$$

If the cycle is performed at constant potential π

$$\oint dg_{max} = 0.$$

Hence, for any cycle at constant potential π

$$g = \oint dg \leqq \oint dg_{max} = 0.$$

Therefore, it is impossible to extract any form of work from a system operating through a cycle at constant value of the corresponding potential. This generalization of the Kelvin postulate is a consequence of the generalized statement of the second law. If all the potentials are constant during a cycle, no work whatsoever can be extracted for use in the surroundings.

GENERALIZATION OF THE CARNOT CYCLE

Let a system operate through a cycle, absorbing heat q_1 reversibly at T_1 and rejecting $-q_2$ reversibly at T_2. The process can be considered

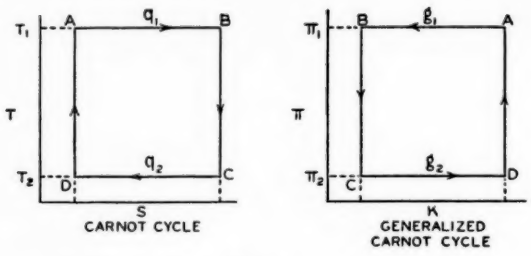

FIG. 1.

to occur in four steps as shown in the diagram: by two reversible isothermal steps AB and CD and two reversible adiabatic steps BC and DA (see Fig. 1).

$$\oint dS = q_1/T_1 + q_2/T_2 = 0. \tag{57}$$

Since $\Delta E = 0$ for the cycle

$$w_{max} = q_{max} = q_1 + q_2.$$

If $T_1 > T_2$ then $q_1 > -q_2$ so that $w_{max} = q_{max} > 0$. Heat is converted into work during the operation of the cycle. If $T_1 < T_2$ then $q_1 < -q_2$ and work is converted reversibly into heat.

$$w_{max} = q_{max} = q_1(T_1 - T_2)/T_1 = q_2(T_2 - T_1)/T_2. \tag{58}$$

These are the conditions obtaining in a Carnot cycle. Now

$$q_{max} = T_1\Delta S_1 + T_2\Delta S_2.$$

But

$$\Delta S_2 = -\Delta S_1.$$

Let

$$\Delta S = \Delta S_2 = -\Delta S_1.$$

Then

$$q_{max} = -(T_1 - T_2)\Delta S. \tag{59}$$

This is the expression for the maximum heat energy available for conversion into other forms of energy in the process of transfer of a charge ΔS from temperature T_1 to T_2. The quantity q_{max} does not depend at all on the nature of the system undergoing the cyclic operation. It depends only on the existence of the temperatures T_1 and T_2 between which the system operates. It is represented by the area $ABCD$ on the diagram with a sign depending on the relative values of T_1 and T_2.

If the system undergoes a cycle in which it performs work g_1 reversibly at π_1 and receives

work $-g_2$ reversibly at π_2 as shown on the diagram, where AB and CD are two reversible changes at constant potential and BC and DA occur reversibly at constant charge, then

$$\oint dK = -g_1/\pi_1 - g_2/\pi_2 = 0. \tag{60}$$

$$g_{max} = g_1 + g_2 = g_1(\pi_1 - \pi_2)/\pi_1 = g_2(\pi_2 - \pi_1)/\pi_2. \tag{61}$$

If $\pi_1 > \pi_2$, then $g_{max} > 0$ so that π-K energy leaves the system. If $\pi_1 < \pi_2$, then $g_{max} < 0$ so that π-K energy enters the system. Now

$$g_{max} = -\pi_1 \Delta K_1 - \pi_2 \Delta K_2.$$

But

$$\Delta K_2 = -\Delta K_1.$$

Let

$$\Delta K = \Delta K_2 = -\Delta K_1.$$

Then

$$g_{max} = (\pi_1 - \pi_2)\Delta K. \tag{62}$$

This is the expression for the maximum π-K work done in the transfer of charge ΔK from potential π_1 to π_2. The quantity g_{max} does not depend on the nature of the system undergoing the cyclic operation; it depends only on the existence of the potential levels π_1 and π_2 between which the system operates. It is represented by the area $ABCD$ on the diagram with a sign depending on the relative values of π_1 and π_2.

That (62) is the expression for the maximum work can be verified by use of the generalized Kelvin postulate. Suppose that some more effective cycle could be found that would perform the same amount of work g_1 at π_1 but would receive less work $-g_2^0$ at π_2. Let this cycle operate the reversible Carnot cycle in reverse. It will extract $-g_2^0$ at π_2 and deliver g_1 at π_1. The reversed Carnot cycle will take up $-g_1$ at π_1 and deliver g_2 at π_2. The net effect of the combined operation is to deliver $g_2^0 + g_2 > 0$ to the surroundings at a constant potential π_2 during a cyclic process. This contradicts the generalized Kelvin postulate.

It may be pointed out that just as a thermodynamic temperature scale can be defined as proportional to the absolute values of q_1 and q_2 in a thermal Carnot cycle, so a thermodynamic potential scale for any π can be defined proportional to the absolute values of g_1 and g_2 in a generalized Carnot cycle. We followed the reverse procedure, introducing the temperature and other potential functions from the start. These functions we now see from (58) and (61) have the property of being proportional to the absolute values of the corresponding charges exchanged in a Carnot cycle.

BRØNSTED'S SYSTEM OF ENERGETICS[1]

Let us write Eqs. (59) and (62) as

$$dq_{max} = (T_2 - T_1)dS, \tag{63}$$

$$dg_{max} = -(\pi_2 - \pi_1)dK, \tag{64}$$

or

$$dw_{max} = -\sum(\pi_2 - \pi_1)dK. \tag{65}$$

We have here represented the maximum heat lost from the surroundings and the maximum work gained in the surroundings during the transfer of infinitesimal amounts of charge from one set of potential levels to another. The maximum energy which the surroundings can lose in these transfers is therefore

$$dE = (T_2 - T_1)dS + \sum(\pi_2 - \pi_1)dK.$$

But since these transfers are accomplished by systems operating through cycles, $dE = 0$, and therefore

$$(T_2 - T_1)dS + \sum(\pi_2 - \pi_1)dK = 0. \tag{66}$$

Equation (66) can be written

$$(T_2 - T_1)dS - (T_2 - T_1)\delta S = -(T_2 - T_1)\delta S - \sum(\pi_2 - \pi_1)dK.$$

But

$$(T_2 - T_1)(dS - \delta S) = T_2(dS_2 - \delta S_2) + T_1(dS_1 - \delta S_1) \geqq 0.$$

Therefore, if we let $Q = (T_2 - T_1)(dS - \delta S)$

$$Q = -(T_2 - T_1)\delta S - \sum(\pi_2 - \pi_1)dK \geqq 0. \tag{67}$$

We see at once the similarity between (67) and (19). Q is interpreted as the energy dissipation during charge transfer. If the transfer of charge occurs reversibly all the charges are transported unchanged in amount from one set of potentials T_1, π_1 to another set T_2, π_2, and $Q = 0$. However, if the transfer is not reversible then entropy is produced and heat Q is evolved. In the reversible transfer of δS and dK, the potentials of the operating system are equal to those of the surroundings and no energy dissipation occurs. But

in the irreversible transfer, the potentials of the system and surroundings are not equal; the transfer of the same quantities of charge between the same potential levels in the system is accompanied by evolution of heat in the system.

Brønsted has made these results the basis of his system of energetics. He considers a "basic energetic" process to consist of the transfer of an amount of charge from one potential to another. The maximum energy of such a process is given by (63) or (64). In a reversible process, basic energetic processes are coupled so that the energy output of one drives another in reverse. The net effect is expressed by the equality sign in (67). This equation Brønsted calls the "work principle." If the process is not reversible, not all the energy of one basic process is utilized in driving others in reverse, but part of the energy is dissipated as heat. This effect Brønsted calls the "heat principle." It is expressed by the inequality in (67). Hence we see that the fundamental postulates of Brønsted's formulation are direct consequences of our treatment. Brønsted's conception of thermodynamics appears entirely within the classical framework of the state of the system. It places needed emphasis on the dissipative aspect of energy processes. But it also is restricted to description of processes between definite states of the system, and is not designed to treat non-static systems with kinetic energy.

THE JOURNAL OF CHEMICAL PHYSICS VOLUME 12, NUMBER 3 MARCH, 1944

Frequency Spectrum of Crystalline Solids. III. Body-Centered Cubic Lattices

ELLIOTT W. MONTROLL AND DAVID C. PEASLEE*
Palmer Physical Laboratory, Princeton University, Princeton, New Jersey
(Received January 3, 1944)

This is a study of the dynamics of a Born-Karman atomic model of a body-centered cubic lattice developed with the assumption that only interactions between nearest and next nearest atomic neighbors are significant. The equations of motion of these systems are derived and the secular equations are given from which one can calculate the frequencies of the crystal's normal modes of vibration. From the secular equations the moments of the frequency spectrum are determined and by solving the "moment problem" the frequency spectrum itself is obtained as a function of the force constants of the lattice. There are two maxima of approximately equal height in the frequency spectrum. Asymptotic expressions are derived for the specific heat of a body-centered cubic lattice which are valid at high and low temperatures.

INTRODUCTION

IN this paper we shall present a theory of atomic vibrations in a body-centered cubic lattice and use this theory to develop equations for the thermodynamic properties of solids with such lattices. First the equations of motion for atoms in body-centered lattices will be derived under the assumptions: (a) that the interatomic forces are sufficiently short ranged so that only interactions between nearest and next nearest neighbors contribute to the total potential energy of the crystal; (b) the temperature of the crystal is low enough so that all internal vibrations are essentially harmonic. Then we shall find the moments of the frequency spectrum and, in the manner described in the other papers of this series,[1] we shall find the frequency spectrum as a function of the lattice constants. From these quantities, expressions will be obtained for the specific heat at high and low temperatures.

I. EQUATIONS OF MOTION

Let us consider a monatomic crystal with a body-centered cubic lattice containing N lattice points in each direction and a total of $2N^3$ atoms. Such a lattice can be conceived of as two inter-

* Present address: Physics Department, Massachusetts Institute of Technology, Cambridge, Massachusetts.

[1] E. Montroll, J. Chem. Phys. **10**, 218 (1942); **11**, 481 (1943).

penetrating simple cubic lattices of equally spaced atoms with a distance a between nearest neighbors on the same simple cubic lattice and a distance $(3/4)^{\frac{1}{2}}a$ between an atom on one simple cubic lattice and its nearest neighbors on the other. Also, let M be the mass of each atom and assume that the interatomic forces are so short ranged that only interactions between nearest and next nearest neighbors are significant.

The mechanical model is indicated in Fig. 1, with lattice points denoted by the subscripts l, m, n—even values corresponding to points on one of the constituent simple cubic lattices and odd values to points on the other. Displacements of an atom from its equilibrium position (defined in such a manner that the potential energy of the system is a minimum and therefore in a state in which no forces act on it) are designated by a vector with components u, v, w taken positive in the direction shown in the figure.

The kinetic energy of the system is

$$T=(M/2)\sum(\dot{u}^2_{l,m,n}+\dot{v}^2_{l,m,n}+\dot{w}^2_{l,m,n}), \quad (1)$$

where the summation is extended over all $2N^3$ atoms of the crystal. Assuming the existence of central forces only, the potential energy of the system can be written

$$V(r_1, r_2, \cdots)=\sum_{i>j=1}^{2N^3} V_{ij}(r_i-r_j). \quad (2)$$

Expanding this function in a Taylor series about the equilibrium coordinates of the molecules, choosing the zero-point energy as the constant term obtained in such a development, remembering that at equilibrium no forces act on any of the atoms, and assuming that displacements from equilibrium are sufficiently small so that their powers higher than the second may be neglected:

$$V(r_1, r_2, \cdots)=\sum_{i>j=1}^{2N^3}(\xi_i-\xi_j)^2V''_{ij}(a_{ij})/2, \quad (2a)$$

where ξ_i is the displacement vector of the ith atom from its absolute zero equilibrium position and $V''_{ij}(a_{ij})$ is the second derivative of the potential energy function evaluated at equilibrium. Since we assumed that the interatomic forces are sufficiently short ranged so that only those between nearest and next nearest neighbors are significant, $V(r_1, r_2, \cdots)$ becomes a function of the two parameters β and δ where

$$3\beta=V''(a_{ij}); \quad \delta=V''(a_{kl}) \quad (3)$$

with i and j a pair of nearest neighbors and k

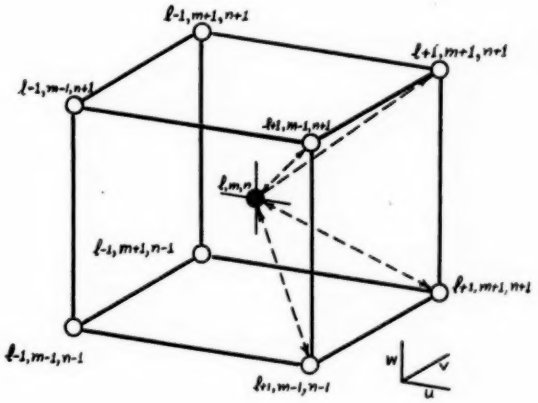

FIG. 1.

and l a pair of next nearest neighbors. In this case

$$V(r_1, r_2, \cdots)=3\beta/2\sum_{\text{nearest}}(\xi_i-\xi_j)^2 + \delta/2\sum_{\substack{\text{next}\\ \text{nearest}}}(\xi_k-\xi_l)^2.$$

Resolving the displacement vectors into vectors u, v, w along the crystal axes (noticing that a factor $1/\sqrt{3}$ is introduced in resolving the vectors u, v, w along the cube diagonal) the total potential energy becomes

$$\begin{aligned}V(r_1, r_2, \cdots)&=(\delta/2)\sum_{l,m,n}[(u_{l,m,n}-u_{l+2,m,n})^2\\ &+(v_{l,m,n}-v_{l,m+2,n})^2+(w_{l,m,n}-w_{l,m,n+2})^2]\\ &+(\beta/2)\sum_{l,m,n}\sum_{b,c=\pm1}[(u_{l,m,n}-u_{l+1,m+b,n+c})\\ &+b(v_{l,m,n}-v_{l+1,m+b,n+c})+c(w_{l,m,n}-w_{l+1,m+b,n+c})]^2.\end{aligned}$$

Substituting these potential and kinetic energy functions into Lagrange's equations for the crystal we have

$$\begin{aligned}0=M\ddot{u}_{l,m,n}&+\delta(2u_{l,m,n}-u_{l+2,m,n}-u_{l-2,m,n})\\ &+\beta[8u_{l,m,n}-\sum_{a,b,c=\pm1}a(au_{l+a,m+b,n+c}\\ &+bv_{l+a,m+b,n+c}+cw_{l+a,m+b,n+c})] \quad (4)\end{aligned}$$

and similar equations to describe the motion of the (l, m, n)th atom in the u and v directions.

If we assume separate periodic solutions for atoms in the two simple cubic lattices:

$$\begin{pmatrix} u_{l+a,m+b,n+c} \\ v_{l+a,m+b,n+c} \\ w_{l+a,m+b,n+c} \end{pmatrix} = \begin{pmatrix} u_0 \\ v_0 \\ w_0 \end{pmatrix} \exp\{i(2\pi\nu t+(l+a)\varphi_1 +(m+b)\varphi_2+(n+c)\varphi_3\} \quad (5)$$

for $a, b, c=0, \pm 2$; and for $a, b, c=\pm 1$:

$$\begin{pmatrix} u_{l+a,m+b,n+c} \\ v_{l+a,m+b,n+c} \\ w_{l+a,m+b,n+c} \end{pmatrix} = \begin{pmatrix} u_0' \\ v_0' \\ w_0' \end{pmatrix} \exp\{i(2\pi\nu t+(l+a)\varphi_1 +(m+b)\varphi_2+(n+c)\varphi_3\}. \quad (6)$$

Here φ_1, φ_2, φ_3 are the phase differences of successive atoms in the three directions of the crystal axes of each simple cubic lattice, and can be written as

$$\varphi_i=2\pi a_i/N \quad i=1, 2, 3 \quad (7)$$

where a_i's are integers such that

$$-N/2\leq a_i\leq N/2,$$

giving an independent solution for each degree of freedom of the system.

Substitution of these solutions into the original differential equation yields

$$\begin{aligned}(8\beta+4\delta\sin^2\varphi_1-4\pi^2\nu^2M)u_0 &\\ -8\beta u_0'\cos\varphi_1\cos\varphi_2\cos\varphi_3 &\\ +8\beta v_0'\cos\varphi_3\sin\varphi_1\sin\varphi_2 &\\ +8\beta w_0'\cos\varphi_2\sin\varphi_1\sin\varphi_3=0. & \quad (8)\end{aligned}$$

Five other similar equations result from these substitutions into Lagrange's equations. Letting

$$\alpha=\beta/4\pi^2M, \quad \gamma=\delta/4\pi^2M \quad (9)$$

$$\begin{aligned} a_{ij}&=8\alpha\cos\varphi_k\sin\varphi_j\sin\varphi_i \quad (i\neq j\neq k)\\ b_i&=8\alpha+4\gamma\sin^2\varphi_i \quad (10)\\ b_0&=8\alpha\cos\varphi_1\cos\varphi_2\cos\varphi_3\end{aligned}$$

the six equations have the form:

$$\begin{aligned}(b_1-\nu^2)u_0-b_0u_0'+a_{12}v_0'+a_{13}w_0'=0,\\ (b_1-\nu^2)u_0'-b_0u_0+a_{12}v_0+a_{13}w_0=0,\\ (b_2-\nu^2)v_0-b_0v_0'+a_{12}u_0'+a_{23}w_0'=0,\\ (b_2-\nu^2)v_0'-b_0v_0+a_{12}u_0+a_{23}w_0=0,\\ (b_3-\nu^2)w_0-b_0w_0'+a_{13}u_0'+a_{23}v_0'=0,\\ (b_3-\nu^2)w_0'-b_0w_0+a_{13}u_0+a_{23}v_0=0.\end{aligned}$$

In order for solutions u_0, v_0, w_0, u_0', v_0', w_0' to exist for this set of simultaneous equations, the determinant of the coefficients of these variables must vanish, i.e.,

$$|U^2|=\begin{vmatrix} b_1-\nu^2 & 0 & 0 & -b_0 & a_{12} & a_{13} \\ 0 & b_2-\nu^2 & 0 & a_{12} & -b_0 & a_{23} \\ 0 & 0 & b_3-\nu^2 & a_{13} & a_{23} & -b_0 \\ -b_0 & a_{12} & a_{13} & b_1-\nu^2 & 0 & 0 \\ a_{12} & -b_0 & a_{23} & 0 & b_2-\nu^2 & 0 \\ a_{13} & a_{23} & -b_0 & 0 & 0 & b_3-\nu^2 \end{vmatrix}=0.$$

By judicious addition and subtraction of rows and columns it is possible to factor this 6×6 determinant into two 3×3 determinants:

$$|U_{\pm}^2|=\begin{vmatrix} b_1\mp b_0-\nu^2 & \pm a_{12} & \pm a_{13} \\ \pm a_{12} & b_2\mp b_0-\nu^2 & \pm a_{23} \\ \pm a_{13} & \pm a_{23} & b_3\mp b_0-\nu^2 \end{vmatrix}. \quad (11a)$$

This is the characteristic determinant which when set equal to zero yields 6 of the $6N^3$ normal modes of the system. It is a function of φ_1, φ_2, φ_3, and therefore of a_1, a_2, a_3. Thus, since each $\{a_i\}$ ranges over

all integers from $-N/2$ to $N/2$, the secular determinant for the entire system becomes

$$|U^2_{\text{total}}| = \begin{vmatrix} U_+^2(-N/2,-N/2,-N/2) & & & & \\ & \cdots & & 0 & \\ & & U_+^2(N/2,N/2,N/2) & & \\ & & & U_-^2(N/2,N/2,N/2) & \\ & 0 & & \cdots & \\ & & & & U_-^2(-N/2,-N/2,-N/2) \end{vmatrix}. \quad (11b)$$

All the $6N^3$ positive roots ν of $|U^2_{\text{total}}| = 0$ correspond to frequencies of the normal modes of vibration of our system.[2]

II. STATISTICAL MECHANICAL DIGRESSION

In a crystal, the number of degrees of freedom and normal modes becomes so enormous that even with the exact solutions to our equations of motion we would be so overwhelmed by detail that it would be difficult to correlate our results with the observations on macroscopic bodies. To alleviate this difficulty we shall review and use several of the well-known equations based on statistical mechanics, which are sufficient to translate our mechanical results into thermodynamic ones.

Before writing down these translation formulae, it is worth saying a few words in answer to some criticism raised against the well-known methods used here.[3] Quantum statistics must be used in our calculations in order to obtain thermodynamic functions that are more accurate than the old Dulong Petit formulae. For this reason it has been argued by some that normal modes calculated according to classical mechanics in the manner discussed in the last section could hardly be employed in the quantum statistical formulae to be used here. This is not the case, for one could determine exactly the same frequencies by starting with Schroedinger's equation as we obtained from Lagrange's equations. By transforming to normal coordinates the Schroedinger partial differential equation is separable and can be shown to have energy levels corresponding to harmonic oscillators whose frequencies are the characteristic values of the matrix of the transformation. The characteristic equation for these characteristic values is exactly (11) and therefore, the classical and quantum mechanical methods of calculating frequencies of normal modes are equivalent.

Another criticism of the standard theory of atomic vibrations in solids is based on the fact that the secular determinants used to calculate frequencies are the same for atoms on the surface of the crystal as for the internal atoms. This is equivalent to setting the boundary conditions on the differential equations in a way that describes physically the wrapping up of a crystal so that opposite faces are connected. Since the number of atoms in the inside of a crystal is of $O(N^3)$ while the number on the surface is only $O(N^2)$, one would expect relative errors of order $(1/N)$ to occur by treating all atoms as equivalent. This can be seen quantitatively by applying a theorem of Ledermann's[4] concerning the characteristic roots of border matrices. This theorem—which states that if n rows of a symmetric matrix are changed in such a manner as to leave the resulting matrix symmetrical, the number of characteristic roots of the matrix in any given interval does not change by more than $2n$—shows that as long as N is large, the distribution of normal modes is not changed appreciably by the assumption of the equivalence of all atoms (including those on the surface) of a crystal.

To change our mechanical results into thermodynamic ones, we employ the equations of Planck and Einstein for calculating thermodynamic properties of a quantized set of oscillators by averaging over all oscillators the contribution of

[2] Vibrations of body-centered lattices have also been studied by P. Fine, Phys. Rev. **56**, 355 (1939). He calculates the frequency spectrum for the case $\gamma/\alpha=2$ by calculating a large random sample of frequencies.

[3] These points have been discussed in greater detail by Born and collaborators, Proc. Phys. Soc. **54**, 362 (1942).

[4] W. Ledermann, Nature **151**, 197 (1943).

a single oscillator to the particular property. For example, the internal energy of a crystal is

$$E=kT\sum_i[\tfrac{1}{2}u_i+u_i/(e^{u_i}-1)], \qquad (12)$$

where $u_i=h\nu_i/kT$ and ν_i is the frequency of the ith normal mode. The heat capacity at constant volume is

$$C_v=k\sum_i u_i^2e^{u_i}/(e^{u_i}-1)^2. \qquad (13)$$

In a crystal there are $O(10^{23})$ normal modes packed into the rather small interval between the smallest and largest frequency, so it is possible to define a continuous function $g(\nu)$ in such a manner that $g(\nu)d\nu$ is the number of normal modes in the interval $\langle\nu, \nu+d\nu\rangle$ at ν. In terms of such a function one can write

$$E=\int_0^{\nu_L}[h\nu/2+h\nu/(-1+\exp(h\nu/kT))]g(\nu)d\nu \qquad (14)$$

where ν_L is the largest frequency. Also,

$$C_v=k\int_0^{\nu_L}g(\nu)(h\nu/kT)^2e^{h\nu/kT}d\nu/(e^{h\nu/kT}-1)^2 \qquad (15)$$

and at high temperatures, if μ_n is the nth moment of $g(\nu)$,

$$\mu_n=\frac{1}{6N^3}\int_0^{\nu_L}\nu^ng(\nu)d\nu=(1/6N^3)\sum_{i=1}^{6N^3}\nu_i{}^n \qquad (16)$$

in a solid with $6N^3$ degrees of freedom, one can expand the internal energy and specific heat in a power series in $1/T$:

$$E/6kTN^3=1-\sum_{n=1}^{\infty}\frac{(-1)^nB_n}{(2n)!}(h/kT)^{2n}\mu_{2n} \qquad (17)$$

and

$$C_v/6kN^3=1-\sum_{n=1}^{\infty}(-1)^nB_n(1-2n)(h/kT)^{2n}\mu_{2n}/(2n)!. \qquad (18)$$

These series converge when $T>h\nu_L/2\pi k$, and the B_n's are the Bernoulli numbers:

$$B_1=1/6;\quad B_2=1/30;\quad B_3=1/42;\quad \cdots.$$

From these formulae it is clear that if the moments of $g(\nu)$ are known, the high temperature series can be evaluated and if $g(\nu)$ itself were known, Eqs. (14) and (15) could be used. It is our aim to determine the first few moments of a body-centered cubic lattice, and to calculate $g(\nu)$ from these moments. The moments will be obtained by taking traces of powers of the matrix of the characteristic determinant (11b), and a polynomial approximation for $g(\nu)$ will be found in the manner suggested in reference 1.

III. COMPUTATION OF MOMENTS

In Eq. (16) we have defined the nth moments of $g(\nu)$ by

$$\mu_n=\sum_{i=1}^{6N^3}\nu_i{}^n/6N^3.$$

To calculate these sums let us examine (11a). $|U_+{}^2|$ and $|U_-{}^2|$ are functions of a_1, a_2, a_3; so let us write them as $|U_+{}^2(a_1, a_2, a_3)|$ and $|U_-{}^2(a_1, a_2, a_3)|$. The matrices $U_+{}^2(a_1, a_2, a_3)$ and $U_-{}^2(a_1, a_2, a_3)$ corresponding to these characteristic determinants each have three characteristic values

$$\nu_i{}^2(a_1, a_2, a_3; +) \quad i=1, 2, 3$$
$$\nu_i{}^2(a_1, a_2, a_3; -) \quad i=1, 2, 3;$$

the roots of $|U_+{}^2|=0$ and $|U_-{}^2|=0$. It is well known that the trace (i.e., sum of diagonal elements) of a matrix is the sum of its characteristic values, and the trace of the nth power of a matrix is equal to the sum of the nth powers of its characteristic values. This means that

$$\text{Trace } U_\pm{}^{2n}(a_1, a_2, a_3)=\sum_{i=1}^{3}\nu_i{}^{2n}(a_1, a_2, a_3; \pm)$$

and

$$\text{Trace } U_+{}^{2n}(a_1, a_2, a_3)+\text{Trace } U_-{}^{2n}(a_1, a_2, a_3)$$
$$=\sum_{i=1}^{3}[\nu_i{}^{2n}(a_1, a_2, a_3; +)+\nu_i{}^{2n}(a_1, a_2, a_3; -)].$$

If we sum both sides of this equation over all values of a_1, a_2, a_3 between $-N/2$ and $N/2$, the right-hand side will yield the sum of the nth powers of all the characteristic values of (11a), or the sum of the $2n$th powers of the frequencies of the normal modes of our body-centered cubic lattice. Therefore

$$\mu_{2n}=\sum_{i=1}^{6N^3}\nu_i{}^{2n}/6N^3$$
$$=\sum_{a_1, a_2, a_3=-N/2}^{N/2}\sum\sum\sum\{\text{Trace } U_+{}^{2n}(a_1, a_2, a_3)$$
$$+\text{Trace } U_-{}^{2n}(a_1, a_2, a_3)\}/6N^3. \qquad (19)$$

The elements in U_+^2 and U_-^2 are trigonometric functions so the sums

$$S_n = \sum_{a=-N/2}^{N/2} \sin^n (2\pi a/N)$$

$$= \begin{cases} 0 & n \text{ odd}, \\ N(2m)!/4^m m!m! & n=2m>0 \end{cases} \tag{20a}$$

$$C_n = \sum_{a=-N/2}^{N/2} \cos^n (2\pi a/N)$$

$$= \begin{cases} -1 & n \text{ odd}, \\ 1+N(2m)!/4^m m!m! & n=2m>0 \end{cases} \tag{20b}$$

will prove useful. They are easily obtained by the methods discussed in the appendix of the first paper of this series.

To proceed further it is convenient to use the formulae given in reference 1 for traces of powers of the 3×3 symmetrical matrix

$$M^2 = \begin{pmatrix} a_{11} & a_{12} & a_{13} \\ a_{21} & a_{22} & a_{23} \\ a_{31} & a_{32} & a_{33} \end{pmatrix}.$$

The first few traces listed there are

$$\text{Trace } M^0 = 3,$$

$$\text{Trace } M^2 = \sum_{i=1}^{3} a_{ii},$$

$$\text{Trace } M^4 = \sum_{i=1}^{3} a_{ii}^2 + 2\sum_{i<j} a_{ij}^2, \quad \text{etc.}$$

These formulae for S_n, C_n, and Trace M^{2n} now enable us to embark on a moment calculating campaign.

Clearly

$$\mu_0 = (1/6N^3) \sum_{a_1, a_2, a_3 = -N/2}^{N/2} \sum\sum (3+3) = 1$$

(henceforth we abbreviate $\sum_{a_1, a_2, a_3 = -N/2}^{N/2} \sum\sum$ by Σ).

From (10) and (11a)

$$\text{Trace } U_+^2(a_1, a_2, a_3) = -3(8\alpha)\cos\varphi_1\cos\varphi_2\cos\varphi_3 + \sum_{i=1}^{3} (8\alpha + 4\gamma \sin^2\varphi_i),$$

$$\text{Trace } U_-^2(a_1, a_2, a_3) = 3(8\alpha)\cos\varphi_1\cos\varphi_2\cos\varphi_3 + \sum_{i=1}^{3} (8\alpha + 4\gamma \sin^2\varphi_i)$$

yielding

$$\mu_2 = (2/6N^3) \Sigma \sum_{i=1}^{3} (8\alpha + 4\gamma \sin^2\varphi_i).$$

Since

$$\sum_{a_i=-N/2}^{N/2} f(a_i) = \sum_{a_j=-N/2}^{N/2} f(a_j), \tag{21}$$

$$\mu_2 = (1/N^3) \Sigma\, (8\alpha + 4\gamma \sin^2 (2\pi a_1/N)]$$

$$= [8N^3\alpha + 4\gamma N^2 S_2]/N^3.$$

However, $S_2 = N/2$, thus $\mu_2 = 8\alpha + 2\gamma$. The calculation of μ_4 is performed in essentially the same way:

$$\text{Trace } U_+^4(a_1, a_2, a_3)$$

$$= \sum_{i=1}^{3} [8\alpha(1 - \cos\varphi_1\cos\varphi_2\cos\varphi_3) + 4\gamma \sin^2\varphi_i]^2 + 2 \sum_{k\neq j,\, i} \sum_{i>j} \sum_{j=1}^{3} (8\alpha)^2 \cos^2\varphi_k \sin^2\varphi_i \sin^2\varphi_j,$$

$$\text{Trace } U_-^4(a_1, a_2, a_3)$$

$$= \sum_{i=1}^{3} [8\alpha(1 + \cos\varphi_1\cos\varphi_2\cos\varphi_3) + 4\gamma \sin^2\varphi_i]^2 + 2 \sum_{k\neq i,\, j} \sum_{i>j} \sum_{j=1}^{3} (8\alpha)^2 \cos^2\varphi_k \sin^2\varphi_i \sin^2\varphi_j.$$

Therefore

$$\text{Trace } U_+^4(a_1, a_2, a_3) + \text{Trace } U_-^4(a_1, a_2, a_3)$$

$$= 2 \sum_{i=1}^{3} [(8\alpha)^2(1 + \cos^2\varphi_1\cos^2\varphi_2\cos^2\varphi_3) + 2(8\alpha)(4\gamma)\sin^2\varphi_i + (4\gamma)^2 \sin^4\varphi_i] + 4 \sum_{k\neq i,\, j} \sum_{i>j} \sum_{j=1}^{3} (8\alpha)^2 \cos^2\varphi_k \sin^2\varphi_i \sin^2\varphi_j.$$

Summing over a_1, a_2, a_3 and remembering (21), we have:

$$\mu_4 = (6/6N^3) \Sigma\, [(8\alpha)^2 + 2(8\alpha)(4\gamma)\sin^2\varphi_1 + (4\gamma)^2 \sin^4\varphi_1 + (8\alpha)^2 \cos^2\varphi_1\cos^2\varphi_2\cos^2\varphi_3 + 2(8\alpha)^2 \cos^2\varphi_1 \sin^2\varphi_2 \sin^2\varphi_3].$$

Since $S_2 = N/2$, $S_4 = 3N/8$, and $C_2 = 1 + N/2$,

$$\mu_4 = 11(8\alpha)^2/8 + (4\gamma)(8\alpha) + 3(4\gamma)^2/8 + O(1/N).$$

In a similar manner we have calculated all the moments up to μ_{14} (of course the odd moments of the distribution of ν's in the interval $-\nu_L$ to $+\nu_L$ are zero). These are exhibited in Table I in the form

$$\mu_{2n}/(8\alpha)^n = \sum_{m=0}^{n} c_{nm}(\gamma/2\alpha)^m. \tag{22}$$

TABLE I. Coefficients c_{nm} of $\mu_{2n}/(8\alpha)^n = \sum_{m=0}^{n} c_{nm}(\gamma/2\alpha)^m$.

n	c_{n0}	c_{n1}	c_{n2}	c_{n3}	c_{n4}	c_{n5}	c_{n6}	c_{n7}
0	1							
1	1	1/2						
2	11/8	1	3/8					
3	17/8	69/32	9/8	5/16				
4	1785/512	37/8	13/4	5/4	35/128			
5	3037/512	9995/1024	35/4	575/128	175/128	63/256		
6	42359/4096	10401/512	181977/8192	925/64	5991/1024	189/128	231/1024	
7	75153/4096	1370901/32768	442351/8192	699209/16384	22337/1024	29939/4096	1617/1024	429/2048

TABLE II. Coefficients u_{jk} of $\mu_{2k}/\nu_L{}^{2k} = \sum_{j=0}^{k} u_{jk}\tau^j$.

k	$u_{0k}\times 2^{21}$	$u_{1k}\times 2^{21}$	$u_{2k}\times 2^{21}$	$u_{3k}\times 2^{21}$	$u_{4k}\times 2^{21}$	$u_{5k}\times 2^{21}$	$u_{6k}\times 2^{21}$	$u_{7k}\times 2^{21}$
0	2,097,152							
1	1,048,576							
2	786,432	−524,288	458,752					
3	655,360	−786,432	737,280	−49,152				
4	573,440	−983,040	1,212,416	−557,056	211,200			
5	516,096	−1,146,880	1,781,760	−1,331,200	603,520	−34,560		
6	473,088	−1,290,240	2,422,272	−2,459,648	1,563,024	−492,192	122,568	
7	439,296	−1,419,264	3,122,560	−3,980,928	3,301,704	−1,642,592	502,397	−22,561

TABLE III. Coefficients c_{ms} of (29). The large number of significant figures is necessary because of the alternate nature of the signs. When the sums are calculated in (29) the first four or five significant figures cancel out.

Coefficient of x^{2s} \ Coefficient of τ^m	0	1	2	3	4	5	6	7
0	0.5079	−11.169	74.288	−179.829	79.331	292.653	−415.736	160.014
1	15.7644	229.220	−2670.052	4,482.010	14,031.725	−48,799.920	49,527.690	−16,801.469
2	−295.8016	2,697.240	−6808.289	96,239.023	−526,675.250	1,067,470.928	−918,350.454	285,624.971
3	2091.4481	−42,993.288	278,265.627	−1,446,771.315	4,781,289.041	−7,960,809.872	6,198,118.208	−1,808,958.152
4	−6,937.2931	187,323.627	−1,386,291.835	6,366,315.906	−17,882,599.351	26,817,158.977	−19,521,822.800	5,426,874.454
5	11,680.7148	−361,246.594	2,824,742.049	−12,349,779.408	31,943,752.827	−44,857,023.934	31,108,254.653	−8,321,207.495
6	−9,661.1765	322,668.729	−2,593,188.532	11,025,764.898	−27,105,235.080	36,371,258.152	−24,314,455.147	6,303,945.072
7	3,115.7088	−108,848.939	887,083.347	−3,700,160.082	8,782,998.327	−11,397,357.637	7,403,131.724	−1,870,401.285

TABLE IV. Coefficients P_n of $\nu_L g(\nu/\nu_L)/6N^3 = \sum P_n\tau^n$.

ν/ν_L	P_0	P_1	P_2	P_3	P_4	P_5	P_6	P_7
0.10	0.6380	−8.6482	47.170	−126.769	171.586	−96.296	−6.288	18.805
.20	0.7824	0.0079	−28.866	75.918	61.312	−396.645	445.801	−157.752
.30	0.6643	10.2900	−93.920	298.844	−436.961	257.127	11.842	−47.104
.35	0.5734	11.6166	−86.086	282.531	−549.662	619.023	−352.883	75.703
.40	0.5490	8.4607	−40.885	127.347	−375.487	655.352	−533.527	159.041
.45	0.6270	1.5551	29.426	−131.019	87.376	246.994	−383.576	149.454
.50	0.7799	−5.9705	93.532	−376.103	637.450	−445.146	52.620	43.675
.55	0.9191	−9.5766	111.796	−448.317	920.140	−992.793	516.991	−98.266
.60	0.9460	−5.9035	59.580	−237.932	622.645	−917.740	657.603	−178.187
.65	0.8368	3.9460	−45.595	199.128	−244.441	−64.175	273.556	−122.145
.70	0.7059	13.0632	−132.692	582.329	−1153.313	1080.611	−437.351	47.950
.75	0.7689	11.2621	−107.810	515.428	−1218.553	1462.577	−852.410	190.077
.80	1.1393	−4.5796	57.415	−161.116	74.477	257.427	−353.301	129.826
.85	1.5408	−18.1758	212.538	−888.060	1748.312	−1723.513	794.551	−125.913
.90	1.3918	3.5765	43.045	−368.419	1041.001	−1370.161	857.749	−206.841
.95	1.4820	45.6436	−394.170	1425.327	−2666.172	2649.747	−1286.683	227.032

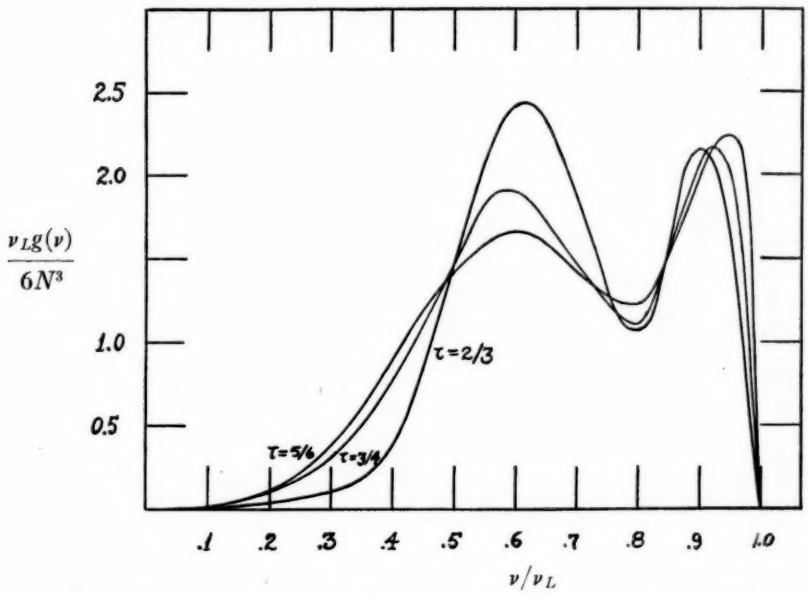

FIG. 2. Frequency spectrum of body-centered cubic lattice. $\nu_L g(\nu)/6N^3$ plotted as a function of (ν/ν_L) for $\tau=2/3,\ 3/4,\ 5/6$.

The largest frequency of the spectrum corresponds to the largest root of (11b). Now Blackman[5] has shown that we may expect maxima to occur in an equation of this type when $\varphi_1,\ \varphi_2,\ \varphi_3$ have some combination of values $0,\ \pi/2,\ \pi$, no combination being excluded except $\varphi_1=\varphi_2=\varphi_3=0$. Accordingly, upon trial we find that at $(0,\ \pi/2,\ \pi/2)$, and $(\pi,\ \pi/2,\ \pi/2)$, (11b) has maximum roots

$$\nu_L^2=4(4\alpha+\gamma). \tag{23}$$

Note that this result is independent of whether $|U_+^2|$ or $|U_-^2|$ is chosen, by virtue of the forms of the a's and b's.

It is more convenient in the work to follow to express the moments as functions of the parameters ν_L^2 and τ, where

$$\tau=4\alpha(2/\nu_L)^2 \tag{24}$$

than in terms of α and γ. In terms of our new parameters

$$\alpha^p\gamma^q=(\tau/4)^p(1-\tau)^q(\nu_L/2)^{2(p+q)}$$

and the moments can be written:

$$\mu_{2k}/\nu_L^{2k}=\sum_{j=0}^{k} u_{jk}\tau^j \tag{25}$$

where the coefficients u_{jk} are exhibited in Table II. In this form the first few moments are:

$$\mu_0=1,\quad \mu_2/\nu_L^2=1/2,$$
$$\mu_4/\nu_L^4=3/8-\tau/4+7\tau^2/32,\quad \text{etc.}$$

IV. FREQUENCY SPECTRUM

First we shall find an approximate asymptotic expression for the frequency spectrum in the range of very low frequencies. It is clear that in order to do this we must find the values of the a_i's which give characteristic roots close to zero. Those which give roots close to zero in $|U_+|^2$ are such as to make $(\varphi_1,\ \varphi_2,\ \varphi_3)$ approach $(0,\ 0,\ 0)$, $(\pi,\ \pi,\ 0)$, $(\pi,\ 0,\ \pi)$, or $(0,\ \pi,\ \pi)$. Those a_i's which give roots close to zero in $|U_-|^2$ are those which make $(\varphi_1,\ \varphi_2,\ \varphi_3)$ approach $(\pi,\ \pi,\ \pi)$, $(0,\ 0,\ \pi)$, $(0,\ \pi,\ 0)$, or $(\pi,\ 0,\ 0)$. In each case (neglecting the off diagonal elements of the determinants) the characteristic determinant reduces to (since $\cos\varphi\simeq 1-\varphi^2/2$ and $\sin\varphi\simeq\varphi$)

$$\begin{aligned}(N\nu/4\pi)^2&\simeq(\gamma+\alpha)a_1^2+\alpha a_2^2+\alpha a_3^2,\\ (N\nu/4\pi)^2&\simeq\alpha a_1^2+(\gamma+\alpha)a_2^2+\alpha a_3^2,\\ (N\nu/4\pi)^2&\simeq\alpha a_1^2+\alpha a_2^2+(\gamma+\alpha)a_3^2.\end{aligned} \tag{26}$$

Each point in $a_1,\ a_2,\ a_3$ space which is enclosed in one of the ellipsoids defined by (26) corre-

[5] M. Blackman, Proc. Roy. Soc. **148**, 324 (1935).

sponds to a frequency whose square is $\leq \nu^2$. Since eight regions of a_1, a_2, a_3 (or φ_1, φ_2, φ_3) space yield (26) and each region gives rise to three ellipsoids, the total number of frequencies whose square is $\leq \nu$ is 24 times the value of one of the ellipsoids given by (26). I.e., if ν is small, the number of normal $\leq \nu$ are

$$N(\nu) \simeq 24(4\pi/3)(N\nu/4\pi)^3/\alpha(\alpha+\gamma)^{\frac{1}{2}}.$$

We defined $g(\nu)d\nu$ as the number of frequencies between ν and $\nu+d\nu$ at ν; thus $g(\nu)=\partial N(\nu)/\partial\nu$, and for very small values of ν,

$$g(\nu)/6N^3 \simeq \nu^2/4\pi^2\alpha(\alpha+\gamma)^{\frac{1}{2}}.$$

From (23) and (24)

$$\alpha(\alpha+\gamma)^{\frac{1}{2}} = \tau(\nu_L/4)^3(4-3\tau)^{\frac{1}{2}}$$

and

$$\nu_L g(\nu)/6N^3 \simeq 16(\nu/\nu_L)^2/\pi^2\tau(4-3\tau)^{\frac{1}{2}}. \quad (27)$$

Using Eq. (35) of the second paper in reference 1, and the moments given in Table II, one can calculate the coefficients a_n of the polynomial approximation

$$G(\nu/\nu_L) = \sum_{n=0}^{7} a_{2n}(\nu/\nu_L)^{2n} \quad (28)$$

of $g(\nu)$. After the introduction of the moments listed in Table II into $G(\nu/\nu_L)$, the approximation of $g(\nu)$ can be written in the more convenient form $(x=\nu/\nu_L)$:

$$\nu_L g(\nu)/6N^3 = \sum_{m=0}^{7} \Big(\sum_{s=0}^{7} c_{ms}x^{2s}\Big)\tau^m, \quad (29)$$

where the coefficients c_{ms} are tabulated in Table III. To facilitate numerical calculations, the sums $\sum_s c_{ms}x^{2s}$ have been computed for several x's in the interval $\langle 0, 1\rangle$ and recorded in Table IV. This table is sufficient for the calculation of $\nu_L g(\nu)/6N^3$ for the values of τ generally found in real crystals. The largest relative error in such calculations probably occurs in the range of low frequencies (i.e., small x's) so in this range one should consider the frequency spectrum to be approximated by the asymptotic expression (27). In Fig. 2 we have plotted $\nu_L g(\nu)/6N^3$ for $\tau=2/3$, $3/4$, and $5/6$ on the basis of Table IV and Eq. (29). As is the case with simple cubic lattices there are two peaks in the frequency spectrum curves. The main difference between the body-centered and simple cubic lattice is to be found in the observation that both peaks carry about equal weight in the body-centered lattice while the high frequency peak is the dominant one in a simple cubic lattice. The curve for $\tau=2/3$ corresponds to the spectrum of metallic tungsten and is in fair agreement with a similar curve determined by P. Fine.[2] Fine's calculations were made by solving a sample of 140 of the determinants (11a) and assuming that the frequency distribution of that sample was representative of the entire distribution.

V. SPECIFIC HEATS

By introducing the eight calculated even moments (Table II) of the frequency spectrum into (18) one can calculate the first eight terms of a power series in inverse temperature for C_v. The first few terms of this series are

$$C_v/6N^3k \simeq 1-(h\nu_L/kT)^2/24 + (h\nu_L/kT)^4(12-8\tau+7\tau^2)/7680-\cdots. \quad (30)$$

At very low temperatures one can derive a T^3 law by combining (15) with (27), yielding

$$C_v/6N^3k \simeq \{16(kT/h\nu_L)^3/[\pi^2\tau(4-3\tau)^{\frac{1}{2}}]\} \times \int_0^{h\nu_L/kT} x^4e^x dx/(1-e^x)^2.$$

As $T\to 0$, the upper limit of the integral $\to\infty$. Since

$$\int_0^\infty x^4e^x dx/(1-e^x)^2 = 4\pi^4/15$$

one obtains the asymptotic expression for C_v

$$C_v/6kN^3 \simeq 64\pi^2(kT/h\nu_L)^3/15\tau(4-3\tau)^{\frac{1}{2}}. \quad (31)$$

The Dependence of the Intensity of Fluorescence on the Composition of a Fluorescing Solution

G. K. ROLLEFSON AND HAROLD W. DODGEN
Department of Chemistry, University of California, Berkeley, California

(Received November 8, 1943)

The fluorescence of solutions of fluorescein and acridone has been studied as a function of (1) the concentration of iodide added with a constant concentration of the fluorescer and (2) the concentration of the fluorescent substance. It is shown that the results are fitted much better by the equation of Stern and Volmer than by that of Perrin. In the absence of a quencher the intensity of the fluorescence observed is given by a function of the concentration which takes into account the following three effects: (1) the absorption of the exciting light by the solution, (2) the absorption of the fluorescent light, and (3) the quenching by the molecules of the fluorescent substance. No other effects needed to be considered for the substances studied.

MANY measurements have been made of the dependence of the intensity of fluorescence in solution on the concentration of the fluorescing substance and also on the concentration of various foreign substances which decrease the intensity. The results have been expressed by means of various equations. Bouchard[1] has used an equation proposed by F. Perrin.[2] For solutions of a fluorescent substance alone this equation is

$$I_0/I = e^{ks}, \tag{1}$$

in which I and I_0 are the intensities of the fluorescence per unit mass of fluorescent substance at concentrations of s and infinite dilution, respectively, and k is a constant. If a quencher is also present the equation is written

$$I_0/I = e^{ks+k'c}, \tag{2}$$

in which the k' is a constant and c is the concentration of the quencher. Stern and Volmer[3] assumed that the quenching depended only on the number of collisions of the quencher molecules with the photoactivated molecule and derived the equation

$$I_0/I = 1+kc. \tag{3}$$

This equation did not attempt to account for any change in intensity with change in the concentration of the fluorescing substance. Frank and Vavilov[4] derived an equation, also dealing only with the action of quenchers, which may be written as

$$I_0/I = (1+kc)e^{k'c}. \tag{4}$$

The exponential factor is introduced to allow for the quenching action of those molecules which happen to be within the necessary sphere of action at the time that the fluorescing molecule is activated. The other factor is determined by the diffusion of the quencher. At low concentrations of the quencher any of these equations will fit the data, but they yield distinctly different results for high concentrations.

In some earlier papers[5] it has been shown that the action of a quencher is influenced by an increase of ionic strength in the same manner as a second-order reaction. In those papers the Stern and Volmer quenching law was assumed since it can be derived by considering that the fluorescence is a first-order reaction and the quenching a second-order reaction and that the intensity of the observed fluorescence is determined by a competition between these two processes. Since Perrin's equation cannot be derived on such a basis it seemed desirable to measure the quenching over a range of concentrations sufficient to establish the nature of the law and thus determine whether or not the process may be treated as a chemical reaction.

[1] J. Bouchard, J. Chim. physique **33**, 51, 127, 232, 325 (1936).
[2] F. Perrin, Ann. de physique **12**, 169 (1929).
[3] O. Stern and M. Volmer, Zeits. f. wiss. Phot. **19**, 275 (1920).
[4] I. M. Frank and S. I. Vavilov, Zeits. f. Physik **69**, 100 (1931).
[5] R. W. Stoughton and G. K. Rollefson, J. Am. Chem. Soc. **61**, 2634 (1939); *ibid.* **62**, 2264 (1940); *ibid.* **63**, 1517 (1941).

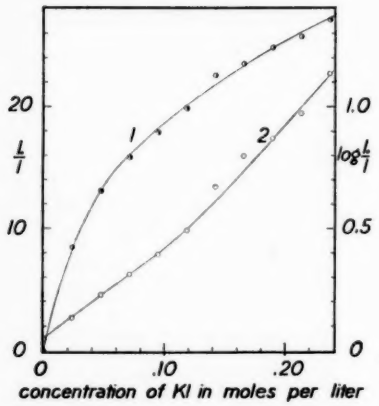

FIG. 1. Test of the quenching laws. Perrin's equation (curve *1*) and Stern and Volmer's equation (curve *2*).

The experiments which have been performed may be divided into two groups. The first experiments were carried out with a constant concentration of the fluorescing substance and various concentrations of the quencher. The second group was with various concentrations of the fluorescer but no quencher. The apparatus used was essentially the same as has been used in the previous work.[5] For excitation the light from a Hereaus type mercury arc was passed through a Corning 586 filter which transmitted only the group of lines around 3660A. The photo-cells used in the measurements were shielded from the exciting light by glass filters which absorbed all wave-lengths less than 4000A.

In order to secure the best test of the quenching equations it is desirable to have as few variables as possible in the system. Since the quenching of the fluorescence of an ion by an ion is markedly affected by changes in the ionic strength it was decided to use acridone as the fluorescing substance in one set of experiments since this is a neutral molecule in solution and it has been shown that the quenching of it by iodide is only slightly affected by large changes in the ionic strength.[5] Another set of experiments was carried out with solutions of fluorescein since the variations of the intensity of the fluorescence with the concentration of the fluorescent substance are quite large in these solutions.

In order to test the various quenching laws stock solutions were prepared of 1.183*M* potassium iodide saturated with acridone and of distilled water saturated with acridone. The solutions needed for the measurements were made by mixing these two in the necessary proportions. The results obtained are represented graphically in Fig. 1. In order to test Eq. (2) we have plotted $\log I_0/I$ *vs.* the concentration of the quencher. In this case it is immaterial whether we plot the ratio of the intensities as measured or convert them into specific intensities since the proportionality factor cancels out in taking the ratio. For Eq. (3) the ratio of the intensities is plotted against the concentration of the quencher. If the correct equation has been chosen the plot should be a straight line. It is apparent that the curve corresponding to Eq. (3) (*2* in the figure) is a straight line up to a concentration of the quencher which quenches ninety percent of the fluorescence and the deviations are not great at larger concentrations. On the other hand, the curve for Eq. (2) shows a marked deviation from linearity at all concentrations. The deviations from linearity shown by the curve *2* may be due to an effect such as is represented by the exponential factor in Eq. (4) but the accuracy of the measurements when the quenching is large is not sufficient to warrant any decision concerning the validity of that equation. Since iodide is one of the most efficient quenchers for acridone it is to be expected that such a factor would be needed in this case if it is going to be needed in any. The fact that the Stern-Volmer equation fits as well as it does leads to the conclusion that the quenching process is correctly viewed as a bimolecular reaction competing with the monomolecular reaction of fluorescence.

Our second group of experiments was designed to study the factors influencing the intensity of fluorescence in the absence of a quencher. Under these conditions the intensity of the fluorescence will depend on (1) the amount of light absorbed by the solute, (2) the amount of the fluorescent light absorbed by the solution, and (3) the quenching of the fluorescence by the molecules of the fluorescent substance. In order to derive an equation for the intensity of fluorescence which will be observed at some point outside the solution let us consider an experimental arrangement such as is shown in Fig. 2. The solution to be studied is contained in a cell with plane parallel ends, the exciting light enters at

one end, and the fluorescence is observed through the other end. A suitable arrangement of filters removes any of the exciting light which is not absorbed by the solution.

If it is assumed that the exciting light is sufficiently monochromatic so that the absorption by the solution obeys Beer's law, the intensity at any point in the solution is given by

$$I' = I_0' \exp(-k_1 cs), \tag{5}$$

in which I_0' is the intensity of the light incident on the cell, k_1 is the absorption coefficient, c the concentration of the solution, and s the distance indicated in the diagram. The amount of light absorbed by a layer ds in thickness is obtained by differentiating (5) which gives

$$dI' = -I_0' k_1 c \exp(-k_1 cs) ds.$$

The intensity of the fluorescence originating in any element of the solution ds in width will be proportional to this quantity dI'. If there is any quenching of the fluorescence by the absorbing molecule the intensity of the light emitted by any such element will be reduced by a factor $1/(1+k_2 c)$ in which k_2 is the quenching constant as defined by Eq. (3). If the observer is far enough from the cell so that the light coming from all parts of the element ds can be considered as having passed through a layer of solution $d-s$ in thickness, then according to Beer's and Lambert's laws the fraction of fluorescent light from any element which reaches the observer is given by $\exp[k_3(l-s)c]$. In this expression k_3 is the absorption coefficient of the solution for the light involved. Since the fluorescent light obtained from solutions is never monochromatic and the absorption coefficient is a function of the wave-length of the light an exact solution of the problem would require that k_3 be determined for each wave-length. However, since it is found experimentally that the absorption is small for all of the wave-lengths in the fluorescent light a reasonable approximation is to use an average value for the whole band. With this approximation we may write for the intensity of the light reaching the observer from the element ds

$$dI = \frac{aI_0' k_1 c}{1+k_2 c} \exp[-k_1 sc - k_3(l-s)c] ds.$$

The factor a is the fraction of the absorbing molecules which would emit light toward the point of observation if there were no quenching. This factor can be considered constant for all positions of ds if the observer is relatively far from the cell. The total observed intensity is obtained by integrating the above expression between the limits 0 and l, the result is

$$I = \frac{aI_0' k_1 c \exp(-k_3 cl)}{1+k_2 c} \int_0^l \exp[-(k_1-k_3)cs] ds$$

$$= \frac{A[\exp(-k_3 cl) - \exp(-k_1 cl)]}{1+k_2 c}. \tag{6}$$

In the final expression A is $aI_0' k_1/(k_1-k_3)$ which is a constant. Similar equations can be derived for observation from the side or front of the solution.

Equation (6) was tested by diluting stock solutions of acridone and fluorescein and measuring the intensity of the fluorescence for each concentration. On account of the low solubility of acridone in water the experiments with that substance were carried out using 95 percent ethyl alcohol as the solvent. The stock solution was $0.00634M$. The stock solution of fluorescein was $0.015M$ with water as the solvent. This solution was also $0.01M$ with respect to sodium hydroxide and $0.2M$ potassium nitrate. These two substances were added in order to keep the fluorescein in the form of the doubly charged ion and to keep the ionic strength constant. Their concentrations were kept constant in the dilution by adding a solution of the same composition except that fluorescein was omitted.

Before testing Eq. (6) as a whole the constants k_1 and k_3 can be determined by direct measurement. The absorption coefficient for the exciting light was determined by filling a cell, such as was used in the study of the fluorescence, with

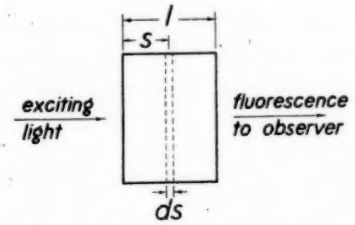

FIG. 2. Experimental arrangement corresponding to Eq. (6).

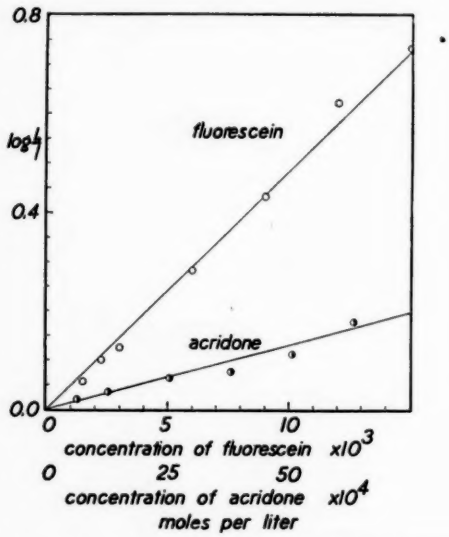

FIG. 3. Dependence of the absorption of the fluorescent light on the concentration of the fluorescer.

solutions of acridone or fluorescein at various concentrations and measuring the intensity of the transmitted light with a photronic cell. The slope of the curve obtained by plotting log (I_0/I) against the concentration of the solution is $k_1 1/2.3$. Good straight lines were obtained for both substances. The absorption coefficient for the fluorescent light was determined in the same way except that the light used was the fluorescence from a thin cell which contained a relatively high concentration of the fluorescent substance. The results are shown in Fig. 3. The fact that the plots of log (I_0/I) *vs.* concentration of the absorbing solution are straight lines justifies the procedure of using a single value for k_3 for each substance.

The self-quenching constant k_2 is obtained from the data obtained by the arrangement shown in Fig. 2. For this purpose Eq. (6) may be put into the form

$$(1+k_2c)/A = [\exp(-k_3cl) - \exp(-k_1cl)]/I.$$

The right-hand member of this equation may be evaluated by means of the previously determined values for k_1 and k_3 and the measurements of the intensity of the fluorescence leaving the cell. If these values are plotted against c the intercept is the value of $1/A$ and the slope is k_2/A. Hence both k_2 and A may be evaluated. The plots of the data are shown in Fig. 4. It is apparent from an inspection of the figure that k_2 is quite small, i.e., there is little self-quenching, for acridone but with fluorescein this effect is of considerable importance. The final values of the constants in Eq. (6) are tabulated for each substance in Table I. Since the intensities of the fluorescence are expressed in arbitrary units, the value of A is in arbitrary units, the other constants are in the units indicated.

The points corresponding to the first two values listed in Table II are outside the range covered by the plot in Fig. 4. Both points fall well above the line shown. This fact may be due to an effect such as is accounted for by the exponential factor in Eq. (4) (the quenching constant is about four times as large as for iodide on acridone and the fluorescein ion is much larger than the iodide ion) but the data at these low intensities are not sufficiently accurate (25 percent as compared to 1 percent for the higher intensities) to warrant any such conclusion. If the data are plotted on the assumption that the self-quenching follows Eq. (1), a curve similar to *1* in Fig. 1 is obtained. In such a plot the data cannot be fitted by any straight line passing

TABLE I. Constants for Eq. (6).

		Fluorescein	Acridone
A	(arbitrary units)	360	874
k_1	(mole^{-1} cm^{-1} liter)	1580	30250
k_2	(mole^{-1} liter)	310	5.84
k_3	(mole^{-1} cm^{-1} liter)	29.5	59.8

TABLE II. Comparison of the observed intensities of fluorescence with those calculated by Eq. (6). Length of the cell used 3.70 cm.

Fluorescein			Acridone		
Molality $\times 10^3$	Obs.	Calc.	Molality $\times 10^4$	Obs.	Calc.
15.0	7	12	63.4	575	576
12.0	15	21	50.7	628	625
9.0	33	35	38.0	685	680
6.0	70	65	25.4	740	739
3.0	140	134	12.7	800	803
2.25	172	166	10.8	810	814
1.5	211	208	8.2	827	827
1.2	230	230	6.34	835	837
0.9	251	254	5.07	843	844
.6	277	275	3.80	855	851
.3	273	262	2.54	855	858
.15	209	195	1.27	850	848
.12	187	171	.634	775	740
.09	150	139	.507	700	681
.06	110	102	.380	610	595
.03	60	56	.254	493	465
			.127	320	277

through the origin as required by the equation. These data therefore furnish additional support for Eq. (3).

The accuracy with which the data are fitted by Eq. (6) is shown by substituting the values for the constants as given in Table I and comparing the calculated and observed intensities. Such a comparison is given in Table II. It is to be noted that A is merely a proportionality factor and does not affect the form of the curve in any way. Since k_2 is the only one of the other constants determined from the intensity measusements it follows that this table shows how well the data can be fitted with what is essentially a one constant equation.

The fact that the calculated intensities fall below the observed ones at low concentrations may be accounted for by a failure to fulfill the condition that the photo-cell used for the observations should be so far from the cell that the factor A is constant. As the concentration of the fluorescent substance decreases the fluorescence spreads more uniformly throughout the cell and the average distance of the source of fluorescence from the photo-cell decreases with a resultant increase in A. The completeness with which the intensity *vs.* concentration curve is fitted on the basis proposed in this paper shows that for the two substances considered no other assumptions are needed. It is possible that with other substances, or even possibly with fluorescein at higher concentrations, it may be necessary to consider other effects such as the formation of more complex molecular species. However, such assumptions should not be introduced until correction has been made for the effects described in this paper which obviously must apply to all systems.

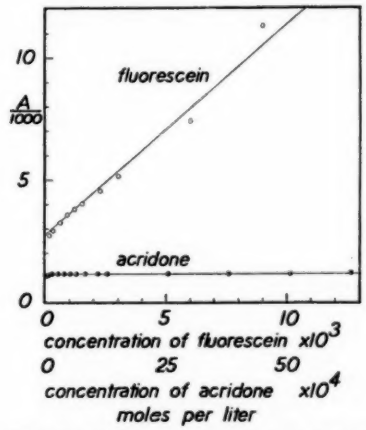

FIG. 4. Plot for determination of A and k_2 in Eq. (6). (The values for acridone were actually determined from a plot on a much larger scale.)

Erratum: Frequency Spectrum of Crystalline Solids. II. General Theory and Applications to Simple Cubic Lattices

[J. Chem. Phys. **11**, 481–495 (1943)]

ELLIOTT W. MONTROLL
Palmer Physical Laboratory, Princeton University, Princeton, New Jersey

PAGE 494, Table IV: Headings should be

$$p_0, p_1\times10^{-1}\cdots p_7\times10^{-7}$$

instead of

$$p_1, p_2\times10^{-1}\cdots p_8\times10^{-7}.$$

Page 495, Eq. (54): Should be a power series in $(h\nu_L/KT)$ instead of in $(kT/h\nu_L)$.

The denominator in the first equation of the second column of page 495 should be

$$/2\pi^2\tau$$

instead of

$$/2\pi^2.$$

Page 495, Eq. (55): The integral above this equation should be

$$4\pi^4/15$$

instead of

$$4\pi^2/15.$$

Letters to the Editor

PROMPT publication of brief reports of important discoveries in physics may be secured by addressing them to this department. The closing date for this department is the third of the month. Because of the late closing date for the section no proof can be shown to authors. The Board of Editors does not hold itself responsible for the opinoins expressed by the correspondents. Communications should not in general exceed 600 words in length.

The Decrease (π) of Free Surface Energy (γ) as a Basis for the Development of Equations for Adsorption Isotherms; and the Existence of Two Condensed Phases in Films on Solids

WILLIAM D. HARKINS AND GEORGE JURA
University of Chicago and Universal Oil Products Company, Chicago, Illinois
February 9, 1944

ONE of the important branches of surface chemistry is that which deals with the adsorption of vapors on the surfaces of solids. In a series of communications from this laboratory, of which this is the sixth, the writers are attempting to develop a treatment of this subject from a new point of view. Our work is based upon the application of equations for adsorption isotherms to the surfaces of about 200 solids, both non-porous and porous. These include a considerable number of catalysts used in the petroleum industry, carbon black, used in rubber, etc., charcoal, and pigments and other crystalline powders. The new point of view is presented below.

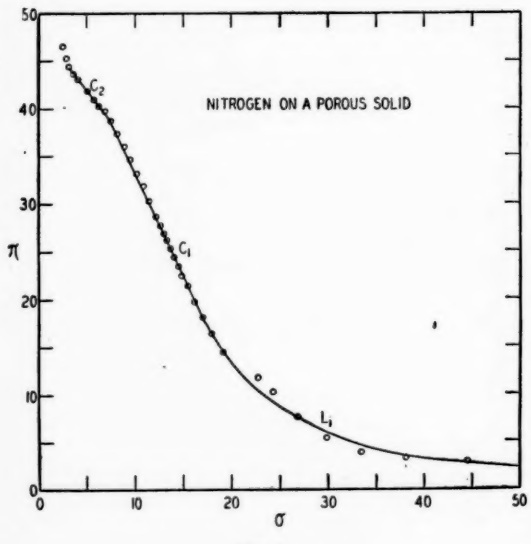

FIG. 1.

1. The treatment of the adsorption of vapors on the surfaces of solids should not be considered as independent of, but as only a part of, a general treatment of the behavior of insoluble and adsorbed films on the surfaces of liquids and of solids of all types.

2. *Since the fundamental property of a surface, which determines the adsorption of a vapor or the spreading of an insoluble film, is the free energy of the surface itself, this quantity should be the fundamental basis of the treatment of this subject.* An adsorption or a spreading process will occur only if it involves a decrease in the free energy of the system. In the adsorption of a vapor at a constant pressure the important decrease in the Gibbs free energy (ζ or F) is that in the free surface energy itself ($-\Delta\gamma=\pi$).

3. Equations which give the pressure-area relations of insoluble oil films on water should apply also to adsorbed films on solids or on liquids. When these are expressed in terms of film pressure and molecular area, they should be capable of conversion into an adsorption isotherm expressed in terms of fugacity (or pressure) and volume (or mass), and this transformation should be made whenever it is profitable to do so.

Thus the equation for a condensed film is

$$\pi=b-a\sigma \tag{1}$$

or the equivalent expression

$$\log\frac{f}{f_0}=B-\frac{A}{v^2}=B'-\frac{A'}{m^2}=\log\frac{p}{p_0}. \tag{2}$$

Here the area of the solid varies as $A^{\frac{1}{2}}$. Both expressions are valid for condensed films on either solids or water, whether they are formed by adsorption or spreading.

Here π, p, and f represent film and gas pressure, and fugacity, respectively, σ represents molecular area, and v or m, volume or mass of material adsorbed.

4. While it may be possible to obtain an adsorption isotherm, which contains only two constants, and which, nevertheless, gives a linear relation that involves two surface phases, such equations apply without a change of constants to only a relatively limited range in each of the phases. The best of these adsorption isotherms, that of Brunauer, Emmett, and Teller, is valid over only the lower pressure region of the condensed phase of the film and the upper pressure region of the intermediate (or possibly expanded) phase. Ours Eqs. (1) and (2) apply to the entire condensed phase (or phases) of the film, but not to any other type of phase.

5. From these considerations a new basis has been adopted for the determination of equations for adsorption isotherms, as illustrated very simply for condensed films by Eqs. (1) and (2), and much less simply in equations for expanded and intermediate films, as developed in the seventh communication.

This consists of considering as impractical attempts to develop a general equation for an entire adsorption isotherm, and in *the determination of a single equation for each of the known phases which exist in oil films on water. A later step is to apply these equations to the pressure (π)-area (σ) relations exhibited by isotherms for films on solids.* In some

cases one equation fits two different phases, but with very different values of the constants. It is found that the equations for insoluble films on water fit equally well for adsorbed films on solids.

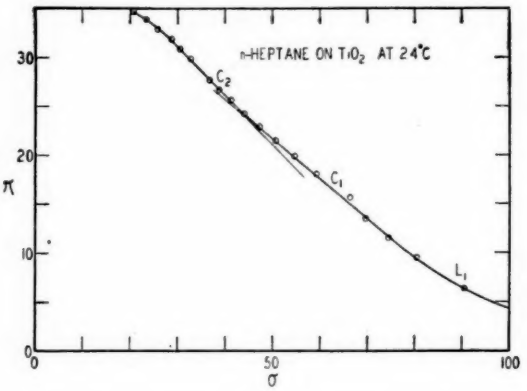

FIG. 2.

TWO CONDENSED PHASES IN FILMS (C_1 AND C_2) ON SOLIDS

The relation expressed by Eq. (1) or (2) is linear. When either of these is applied to films on solids it is often found that *the plot obtained exhibits two straight lines such as to indicate the existence in the film on the solid of two condensed phases with a second-order transition, and thus an absence of a latent heat, between them* (Figs. 1 and 2). The transition between the intermediate (L_i) and the condensed film (L_c) may be considered as of the third order.

Examples of this are found in films of propyl alcohol on barium sulfate or anatase (TiO_2), and of nitrogen on certain catalysts used in the petroleum industry, or on certain charcoals.

The only previously recognized *phase* on solids is the gaseous film.

Equations for the Pressure (π)-Area (σ) Relations (Isotherms) of Liquid Expanded and Intermediate Monolayers on Water

GEORGE JURA AND WILLIAM D. HARKINS
University of Chicago and Universal Oil Products Company, Chicago, Illinois
February 9, 1944

IN earlier communications the writers have given equivalent equations for the isotherms of condensed films either adsorbed or spread on the surfaces of liquids or solids. These are

$$\pi = b - a\sigma, \tag{1}$$

$$\log \frac{f}{f_0} = B - \frac{A}{V^2} = B' - \frac{A'}{m^2} = \log \frac{p}{p_0}. \tag{2}$$

Here Eq. (1) is so simple that its form is obvious.

This is not at all true in the case of the liquid expanded or liquid intermediate phases on an aqueous subphase, since no earlier equation which fits their behavior has ever been developed.

In this connection the well-known equation of Langmuir,[1] a simplified van der Waals equation, which is supposed to exhibit the pressure (π)-area (σ) relations of liquid expanded monolayers, may be considered. It is

$$(\pi - \pi_0)(\sigma - \sigma_0) = kT. \tag{3}$$

However, endeavors to fit this equation to any of the very large number of determinations in this laboratory of the pressure-area relations of the liquid expanded phase have shown that no equation of this type represents the data at all well.

Since the equations for the compresssbilities (κ) of the expanded and intermediate phases are much simpler than those for the film pressures (π), our method of procedure is to obtain first the equation for the compressibility, where $\kappa = -(1/\sigma)(\partial\sigma/\partial\pi)_{T,p}$, and then to integrate the equation to obtain that for π.

A study of the data for the liquid expanded and intermediate films of insoluble materials on aqueous subphases has shown that the following equations for the compressibility represent adequately the experimental data:
(1) Liquid expanded phase:

$$\kappa = \frac{1}{a\sigma - b} \tag{4}$$

where the constants a and b have positive signs. On integration the π, σ relationship is found to be

$$\pi = c + a\sigma - b \ln \sigma. \tag{5}$$

(2) Intermediate phase:

$$\kappa = -a + (b/\sigma). \tag{6}$$

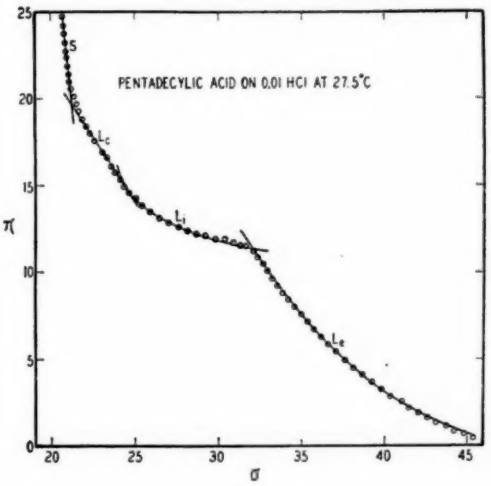

FIG. 1.

The constants a and b are again considered to be positive. The pressure-area relationship found on integration is

$$\pi = c - 1/a \ln (a\sigma - b). \tag{7}$$

At the present time these relationships are to be considered empirical. The only theoretical significance apparent at present is that obtained by comparing the compressibility to that of the condensed phase. Here the compressibility is known to be

$$\kappa = -a/\sigma. \tag{8}$$

The normal succession of phases, when the three appear by compression is (1) the expanded, (2) the intermediate, and (3) the condensed. The compressibilities of the film, in the same order, are $-(1/a\sigma - b)$, $-a+(b/\sigma)$, and $-a/\sigma$. Insufficient work has been done, as yet, to determine whether the constants a and b have theoretical significance. Figure 1 shows the application of the above equations to the liquid expanded and intermediate films of pentadecylic acid at 27.5° C on water.

[1] I. Langmuir, J. Chem. Phys. **1**, 762 (1933).

The Existence of Expanded and Intermediate Phases in Films on Solids

GEORGE JURA AND WILLIAM D. HARKINS
University of Chicago and Universal Oil Products Company, Chicago, Illinois
February 9, 1944

IN this communication it is shown that the equations developed for insoluble monolayers on water in the liquid expanded and intermediate phases are valid for certain films adsorbed on the surfaces of non-porous and porous solids. From this evidence the conclusion is reached that these two non-condensed phases exist in films on the surfaces of solids as well as on liquids. This conclusion is based on work with adsorbed films of butane on porous solids (catalysts) at 0° C. These exhibit even the second-order transition between the two phases. The pressure-area diagram for one of these solids is shown in Fig. 1.

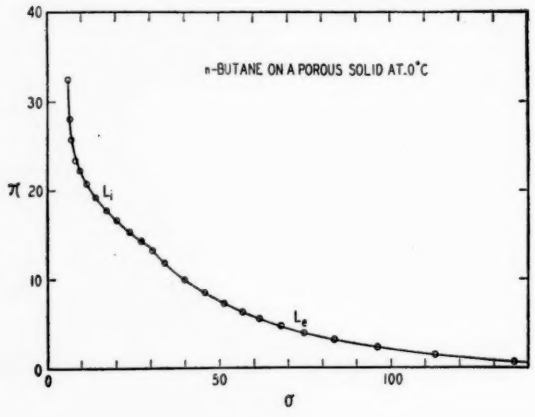

FIG. 1.

The equation obtained for the adsorption isotherm of the expanded phase, as obtained from Eq. (5) of the preceding paper, is

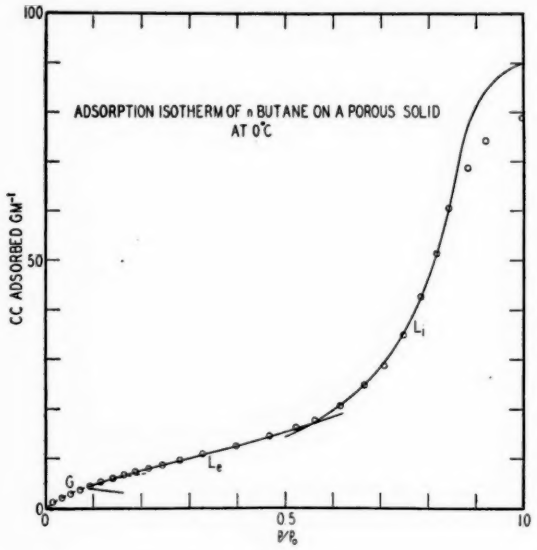

FIG. 2.

$$\log_{10} p = C + \frac{aA}{2.303B}\cdot\frac{1}{v^2} - \frac{b}{B}\cdot\frac{1}{v} \tag{8}$$

while that for the intermediate phase is

$$\log_{10} p = C + \frac{aA}{2\times 2.303B}\cdot\frac{1}{v^2} - \frac{b}{a^2AB}\log\frac{aA-bv}{v}. \tag{9}$$

In these equations p is the equilibrium pressure, v the volume of gas adsorbed per gram, a and b the constants in the compressibility equation,

$$A = 10^{16}\times 22{,}410\Sigma/6.023\times 10^{23}, \text{ and } B = RT/22{,}410\Sigma.$$

In the expressions for A and B, Σ is the specific area of the solid in $cm^2\ g^{-1}$. The application of these equations to the adsorption data is shown in Fig. 2. Actually three phases are shown, the gaseous, the expanded, and the intermediate. The agreement between the observed and calculated values is well within experimental error except at very high pressures. Here the deviation is undoubtedly due to the fact that the pores are limiting the amount of material which is being adsorbed.

Thermodynamics of Heterogeneous Polymer Solutions

PAUL J. FLORY
Goodyear Research Laboratory, The Goodyear Tire and Rubber Company, Akron, Ohio
February 11, 1944

THE equations derived by Huggins[1] and the writer[2] to represent the thermodynamics of polymer solutions take no account of the heterogeneity of the polymer. This limitation is of no consequence in the treatment of osmotic pressure, vapor pressure lowering, etc., in systems composed of a single polymer-containing phase, provided that the *number average* degree of polymerization is employed.

In dealing with solubility and fractional precipitation (or solution) of polymers composed of numerous species differing in molecular size, the above equations obviously are inadequate.

The previously employed statistical mechanical procedures can be readily applied to solvent-heterogeneous polymer systems. The following expression is derived for the entropy of mixing of n moles of solvent with N_1, N_2, N_3, $\cdots$ moles of polymer molecules of 1, 2, 3, $\cdots$ units, respectively, each existing initially as a pure component in which the molecules are in disordered configurations

$$\Delta S^* = -R[n \ln v_1 + \Sigma(N_x \ln v_x)], \quad (1)$$

where v_1 and v_x are the volume fractions of solvent and x-mer, respectively. Partial differentiations with respect to n and to N_x yield the partial molal entropies of the components. Combining these with van Laar partial molal heat of mixing terms, μRTv_2^2 and $\mu xRT(1-v_2)^2$, the partial molal free energies

$$\Delta\bar{F}_1 = RT[\ln(1-v_2) + (1-1/\bar{x}_n)v_2 + \mu v_2^2], \quad (2)$$

$$\Delta\bar{F}_x = RT[\ln v_x - (x-1)(1-v_2) + v_2(1-x/\bar{x}_n) + \mu x(1-v_2)^2] \quad (3)$$

are obtained, where v_2 is the volume fraction of all polymer species and $\bar{x}_n$ is their number average number of units per polymer molecule.[3] The precipitation of a polymer from solution occurs with the formation of two liquid phases,[2] one richer in the polymer constituent than the other. The higher polymers occur preferentially in the more concentrated phase (precipitate) which actually may consist largely of solvent.[2] Analysis of solubility and fractionation of heterogeneous polymers requires the introduction of the conditions for equilibrium between the coexisting phases, i.e.,

$$\Delta\bar{F}_1 = \Delta\bar{F}_1', \quad (4)$$

$$\Delta\bar{F}_x = \Delta\bar{F}_x', \quad (5)$$

where the unprimed terms refer to the dilute phase and the primed terms to the more concentrated (precipitated phase). Substituting (3) in (5) there is obtained

$$v_x'/v_x = \exp(\alpha x) \quad (6)$$

where

$$\alpha = v_2(1-1/\bar{x}_n) - v_2'(1-1/\bar{x}_n') + \mu[(1-v_2)^2 - (1-v_2')^2], \quad (7)$$

assuming μ to be the same in both phases.

Equation (6) expresses the form of the partition of polymer species between the two phases as a function of their size x. However, the separation factor α is not an explicit function of independent variables. Complete analysis of the partition of a polymer of known distribution of species requires use of the following approximate equation, obtained from (2) and (4),

$$(v_2'-v_2)^3/12(1-v_2'-v_2) \leqq \frac{\alpha}{2}(v_2'+v_2) - v_2'/\bar{x}_n' + v_2/\bar{x}_n \quad (8)$$

and the necessary condition

$$\Sigma[v_x^0 e^{\alpha x}/(1+re^{\alpha x})]/\Sigma[v_x^0/(1+re^{\alpha x})] = v_2'/v_2, \quad (9)$$

where v_x^0 is the initial volume of x-mer and r is the ratio of the volumes of the two phases.

These equations are not soluble in terms of the independent variables μ, the initial distribution (v_x^0's), and total concentration. It is feasible, however, to substitute assumed values of r and α in (9) and in equations not included here for the number averages x_n and x_n'. Equation (8) can then be solved for v_2 and v_2', and μ can be obtained from (7).

The application of these equations to solubility and fractionation of high polymers will be published in greater detail when time permits.

[1] M. L. Huggins, J. Phys. Chem. **46**, 151 (1942); Annals N. Y. Acad. Sci. **43**, 1 (1942); Ind. Eng. Chem. **35**, 216 (1943).
[2] P. J. Flory, J. Chem. Phys. **10**, 51 (1942).
[3] The entropy expression (1), or its analog for a homogeneous polymer, fails to yield correct entropies in the region of dilute solutions. (Paper presented by the writer before the Pittsburgh Meeting of the American Chemical Society, September, 1943.) Huggins (reference 1) has shown that free energy expressions corresponding to (2) and (3) reproduce experimental data satisfactorily. It is necessary, however, to regard μ as an empirical parameter only part of which arises from the heat of mixing. Thus, although the theory is at fault in dilute solutions, Eqs. (2) and (3) should reproduce satisfactorily the actual free energies of the components throughout the concentration range.

Condensation and Supersaturation of Adsorbed Phases

HANS M. CASSEL
Research Laboratory, Dearborn Chemical Company, Chicago 16, Illinois

February 15, 1944

IT is well known that in the derivation of Langmuir's adsorption isotherm the interaction of neighboring adatoms has been neglected. Consequently, the equation of state of the monolayer corresponds to that of a compressed gas above its critical point. It is remarkable that this holds, no matter what the magnitude of the adsorption energy. This being so, the question naturally arises: How can the recently developed extensions of the simple Langmuir mechanism to the treatment of multilayers in the adsorption of vapors account for the final liquefaction of the adsorbate?

Let us write the Emmett-Brunauer-Teller[1] adsorption isotherm:

$$\Gamma = \Gamma_m cp P/(P-p)[P+(c-1)p],$$

where Γ designates the surface density, Γ_m that of a complete monolayer, p the equilibrium, and P the saturation pressure of the adsorbate. Let us eliminate the surface density by applying Gibbs' equation:

$$-d\sigma = \Gamma RT d \log p$$

where σ is the sum of interfacial tension of the adsorbent and surface tension of the film. Hence integration gives the film pressure:

$$\sigma_0 - \sigma = F = \Gamma_m RT \log \frac{P+(c-1)p}{P-p}.$$

So we have to conclude that the surface tension of the finally built-up, presumably liquid film would be negative.

This catastrophe is obviously due to the disregard of lateral cohesion in the design of the film model.

In considering the mutual attraction of adatoms, cluster formation and phase transitions can be anticipated as has been repeatedly discussed.[2] Accordingly, the adsorption isotherm of a vapor must show a discontinuity, of course also in case of perfect wetability. Then, depending on the free energy of nucleus condensation, metastable mono- or multilayers should be observed. It is very likely that the hysteresis in capillary condensation[3] represents a supersaturation phenomenon of this kind.

[1] S. Brunauer, P. H. Emmett, and E. Teller, J. Am. Chem. Soc. **60**, 309 (1938).

[2] J. Frenkel, Zeits. f. Physik **26**, 117 (1924); H. Cassel, Ergeb. d. exakt. Naturwiss. **6**, 114 (1927); N. Semenoff, Zeits. f. physik Chemie **B7**, 471 (1930); I. Langmuir, J. Chem. Phys. **1**, 3 (1933); A. Frumkin, Acta Physicacimica U.S.S.R. **9**, 313 (1938); W. Band, J. Chem. Phys. **8**, 178 (1940).

[3] H. B. Weiser, W. O. Milligan, and J. Holmes, J. Phys. Chem. **46**, 582 (1942); P. H. Emmett and T. W. DeWitt, J. Am. Chem. Soc. **65**, 1253 (1943); L. H. Cohan, *ibid*. **66**, 98 (1944).